Wind variability over the northern Indian Ocean during the past 4 million years – insights from coarse aeolian dust (IODP Exp. 359, site U1467, Maldives)

Manuscript Details

Manuscript number	PALAEO_2019_244_R1
Title	Wind variability over the northern Indian Ocean during the past 4 million years – insights from coarse aeolian dust (IODP Exp. 359, site U1467, Maldives)
Article type	Research Paper

Abstract

The lithogenic fraction of carbonate drift sediments from IODP Exp. 359 Site U1467 (Maldives) provides a unique record of atmospheric dust transport over the northern Indian Ocean during the past 4 Myr. Grain-size data provide proxies for dust flux (controlled by source area aridity) as well as wind transport capacity (wind speed). Entrainment and long-range transport of dust in the medium to coarse silt size range is linked to the strength of the Arabian Shamal winds and the occurrence of convective storms which prolong dust transport. Dust flux and the size of dust particles increased between 4.0 and 3.3 Ma, corresponding to the closure of the Indonesian seaway and the intensification of the South Asian Monsoon. There is no clear trend in dust flux between 3.3 and 1.6 Ma, whereas wind transport capacity decreased. Between 1.6 Ma and the Recent, dust flux increased and shows higher variability, especially during the last 500 kyr. Transport capacity increased between 1.2 and 0.5 Ma and slightly decreased since then. Frequency analysis shows that dust transport varies on orbital timescales, with eccentricity control being the most prominent (400 kyr throughout the record, 100 kyr between 2.0 and 1.3 Ma, and since 1.0 Ma). Higher frequency cycles (obliquity and precession) are more pronounced in wind transport capacity than in the amount of dust. This indicates that the amount of coarse dust in sediments from the Maldives as a far-field site is more prone to changes in transport mechanisms than to changes in dust source-area aridity.

Keywords	climate archive; dust; grain size; carbonate drift; South Asian Monsoon; Shamal wind
Manuscript region of origin	Europe

Corresponding Author	Sebastian Lindhorst
Corresponding Author's Institution	Institute of Geology, University of Hamburg
Order of Authors	Sebastian Lindhorst, Christian Betzler, Dick Kroon

Suggested reviewers	Cynthia Twohy, charles bristow, Joseph Prospero, peter demenocal, Jan-Berend W. Stuut

Submission Files Included in this PDF

File Name [File Type]

Cover letter.pdf [Cover Letter]

Reply to the reviewers comments.pdf [Response to Reviewers]

Lindhorst et al. - Manuscript Indian Ocean Dust_Rev1.docx [Revised Manuscript with Changes Marked]

Lindhorst et al., Highlights_Rev1.docx [Highlights]

Lindhorst et al. - Manuscript Indian Ocean Dust_Rev1_no marks.docx [Manuscript File]

Lindhorst et al., Fig. 1_Rev1.tif [Figure]

Lindhorst et al., Fig. 2.tif [Figure]

Lindhorst et al., Fig. 3_Rev1.tif [Figure]

Lindhorst et al., Fig. 4.tif [Figure]

Submission Files Not Included in this PDF

File Name [File Type]

Lindhorst et al_Supplementary Material_Rev1.xlsx [Table]

To view all the submission files, including those not included in the PDF, click on the manuscript title on your EVISE Homepage, then click 'Download zip file'.

Research Data Related to this Submission

There are no linked research data sets for this submission. The following reason is given:
Data are available in the supplemental material. In addition, they will be available from the database Pangäa.

Universität Hamburg
DER FORSCHUNG | DER LEHRE | DER BILDUNG

cen

UHH · CEN · Institut für Geologie
Bundesstraße 55 · 20146 Hamburg

Editor Palaeogeography, Palaeoclimatology, Palaeoecology

Dr. Sebastian Lindhorst
Universität Hamburg
CEN Centrum für Erdsystemforschung
und Nachhaltigkeit · Institut für Geologie
Bundesstraße 55; 20146 Hamburg

Tel. +49 (0)40 42838-5024
Fax +49 (0)40 42838-5007
sebastian.lindhorst@uni-hamburg.de

Datum 25.08.2019

Dear Editor,

Please find our revised manuscript entitled "*Wind variability over the northern Indian Ocean during the past 4 million years – insights from coarse aeolian dust (IODP Exp. 359, Site U1467, Maldives)*" (Paleo_2019_244) for re-submission to the **special volume "IODP 359 - Maldives"** edited by Jeremy Young.

In revising our manuscript, we have carefully addressed all of the reviewer's comments. Please refer to the attached document "Reply to the reviewers comments.pdf" for details.

You will find that the list of authors has been changed. In the course of the decision to remove the Sr-Nd data from the manuscript and to postpone their publication until more data are available, Dr. Liviu Giosan (who was in charge for the Sr-Nd data) resigned from the list of authors (see rebuttal letter for details).

We herewith confirm that the manuscript presents data which are original and new and not published nor under consideration for publication elsewhere. All authors are free of competing interests.

I look forward to hearing from you soon.

Sincerely yours,

Sebastian Lindhorst (corresponding author)

Comments to the revision of our manuscript entitled "Wind variability over the northern Indian Ocean during the past 4 million years – insights from coarse aeolian dust (IODP Exp. 359, Site U1467, Maldives)" (PALAEO_2019_244).

We thank the reviewers for their thorough and constructive reviews. All changes to the manuscript in reply to the reviewer's comments (***set in italic***) are described in the following (**blue text below**) and are **marked in red** in the revised form of the manuscript. Line numbers refer to the original version of the manuscript. All comments have been numbered consecutively to improve clarity.

In revising the manuscript, we found that many of the reviewer's comments were on the radiogenic isotope data and the methods involved in their determination. We follow most of the comments and agree that the isotope data set presented is small and that results remain ambiguous regarding the provenance of dust deposited in the Maldives area and would require a much more in-deep discussion. However, these data were never intended to stand in the focus of this manuscript which is on the grain-size distribution of dust in the medium to coarse silt range. Based on this, and on discrepancies on their interpretation, one author (Liviu Giosan) suggested removing these data (and himself as their author) from the manuscript and to postpone their interpretation to a future report focused on dust provenance, once more data have been measured (already underway). As a result, the manuscript has been adjusted in parts and Liviu Giosan has been removed from the author list.

Reviewer 1

1. *In describing the modern setting for atmospheric circulation and dust delivery to the region, please make sure to include key citations such as Prospero et al 2002 (doi.org/10.1029/2000RG000095) on the modern eolian sources and transport mechanisms across the region.*

Thank you for pointing us to this paper. We have included the reference in the introduction as well as the discussion, as suggested.

2. *Other important papers you should consider including in the introduction as well as while discussing your data include:*

a) *Aeolian delivery to Ulleung Basin, Korea (Japan Sea), during development of the East Asian Monsoon through the last 12 Ma. https://doi.org/10.1017/S001675681900013X*

b) *Monsoon-driven Saharan dust variability over the past 240,000 years. DOI: 10.1126/sciadv.aav1887*

We have studied both papers and have decided to incorporate them as suggested. **a)** presents a study from the Japan Sea, where dust flux is controlled by different mechanisms than in the northern Indian Ocean. Nevertheless, the larger scale atmospheric framework is influenced by similar mechanism which makes this paper interesting also for our case. **b)** however, focusses on Saharan dust and investigates the cyclic variability of dust entrainment and the reliability of former studies. This study found that – in contrast to our findings – dust flux is rather controlled by higher frequency changes in insolation (precession and obliquity) than the glacial-interglacial variability of global climate. We have incorporated this (very new)

paper in our manuscript for completeness but prefer not to change our interpretation with this regard.

3. *A question that comes to mind is, what is the (or is there any) influence from latitudinal migration of the Jet in alternating the source and transport mechanism of dust delivery? The Shamal's are a component of the larger atmospheric circulation that also includes the Afro-Asian (winter and summer) monsoon systems, and the Jet is part of the system. Would this be worthy of mentioning in the introduction, or does this part of the system primarily impacts the Japan Sea and Western Pacific deposits?*

This is indeed an interesting question. However, without having high-resolution provenance data, it seems impossible to assess the influence of changes in the larger, hemisphere-scale circulation patterns onto dust supply. At this stage, this seems to be beyond our very limited dataset. We therefore would prefer not to expand the introduction with this regard

4. *I also think it would serve the manuscript better to expand the introduction to include a more comprehensive reference to the state-of-the-art knowledge of modern, millennial and orbital changes in the sources and input of dust to northern Indian Ocean and the Arabian Sea. Frank's pioneering work and others from the 80s and 90s are mentioned in the intro and referred to later but I think this dataset will be more appreciated if its contribution is expressed in the context of the literature upfront in the introduction, with consideration for both modern and glacial/interglacial timescales.*

In principal, we agree that a broader and more in-depth view on previous work on the cyclic variability of dust transport would improve the introduction. However, our dataset lacks the temporal resolution to provide a detailed study on high-frequency cyclicities. With a temporal sample interval of 5.3 ka (median) changes on millennial time scales are not visible and even the precessional (19 and 23 ka) band is at the very limit, as in some parts the temporal resolution is lower (compare L218-222). Furthermore, as you already mentioned (comment 8), there is some uncertainty in the age model due to the approach we have used for tuning. Due to this, we decided to mention but not to emphasize the analysis of cycles and periodicities. This, however, is still in our mind and a higher resolution data set might bear this potential in the future. Summarizing, we would prefer not to expand the introduction with regard to cyclic changes in the dust cycle.

5. *The methods section for Sr-Nd isotope analysis should be more explicit with regard to the details of the chemistry used, especially considering the presence of coral fragments? Citing Bayon's method should be accompanied by more details of the approach used in the lab with more on what measures were taken to minimize contamination from coral/in situ carbonate fragments of all sizes with the potential to skew the Sr isotope signature of the lithogenic fraction.*

The Sr-Nd data has been removed from the manuscript and will be presented in a separate manuscript, once more data are available; see above.

6. *Please provide the 2sigma/95%ci uncertainties on all isotope measurements and eNd values. How was the external precision "estimated" at such ppm levels? Traditionally, the analytical precision of each isotope measurement is presented. In the absence of a large dataset that can hint to potential trends or clusters, interpreting data points in the Sr-Nd isotope space that have overlapping analytical uncertainties and/or fall within the external reproducibility of the analysis calls for additional caution.*

With the uncertainties demonstrated, one can then begin to discuss if the Sr isotopes show a relatively narrower range compared with Nd isotopes, and whether this represents the eolian/source signature. I don't see evidence that the Sr isotope data is skewed by the seawater signature but more information would provide reassurance.

> The Sr-Nd data has been removed from the manuscript and will be presented in a separate manuscript, once more data are available; see above.

7. *Beyond the analytical aspect, I think the relatively small Sr-Nd dataset presented here should be discussed with emphasis as being preliminary data, and less as conclusively pointing to the provenance of dust to the Maldives for this incredibly long record, which shows great potential for a high-resolution investigation. For example, the contribution of the mighty Indus to the fine lithogenic fractions cannot be entirely discounted in my opinion with the current data, even though prior studies have shown lateral vs. vertical sedimentation rates calculated using different methods generally agree on eolian deposition dominating in the eastern Arabian Sea region. In any case, I would remain focused in this manuscript on the implications of the particle size analysis, intrigued by the (limited) geochemical isotope data.*

> As stated above, based on this comment and others, we have decided to remove the Sr-Nd data from the manuscript and to focus on the grain-size record. We agree that the isotope data are promising and intend presenting these data in a separate manuscript, once more data are available (see above).

8. *Please also include an estimate of the uncertainty associated with the age model established from correlating the bulk grain-size data of Site U1467 with the sea-level data, especially since apparently a subjective approach was employed for this task?*

> Pattern fitting of curves is always subjective to a certain degree, providing quantitative error ranges is therefore misleading in our opinion. Nevertheless, given that the sedimentation rates are expected to be strongly driven by the sea-level controlled input of fines in the bulk sediment, this aspect in our opinion has also absolutely to be taken into account when refining the depth to age correlation. We therefore believe that our approach is valid.

9. *Measuring particle sizes in sediments is inherently challenging. While I understand an established method was used, it would be reassuring if the authors elaborate on their level of confidence that in the process of preparing the samples, the particle data measurements remained representative of the originally deposited samples. How did the authors address the potential disintegration of aggregate particles prior to the analysis, considering the main arguments of the manuscript hinge on bulk grain size data?*

> Prior to grain-size measurement, all samples were dispersed in water using ultrasonic and 0.05% $Na_4P_2O_7 \times 10\ H_2O$ (tetra-sodium diphosphate decahydrate) as dispersing agent (see L166f). For the terrigenous fraction, this and the intensive chemical treatment in the course of carbonate and opal dissolution, ensures that all particle aggregates were disintegrated prior to measurement (with the exception of early cemented particles, see L204-208). This has also been checked by means of binocular microscope (L163ff). For bulk grain-size data, by contrast, we cannot completely exclude that a very few aggregate particles survived until

measurement. However, in our opinion, this is very unlikely to have influenced our dataset as only the portion of bulk mud (< 63 µm) is used for this study.

Reviewer 2

10. ***a)*** *(…)I am wondering how you define the grain-size "classes" you are working with. Why do you not use the full grain size spectrum but only bulk%mud? How the grain size distributions are look like? When you talk about coarsening or fining of the record, the first thing I would look at is the mean grain size, which is not shown. Any reason for that?* ***b)*** *You talk about coarse and even giant dust particles, which are a lot bigger than 63 µm, so why the restriction to below 63µm?*

First of all, we have to clarify that there are grain-size data for both, carbonate dominated bulk samples and the terrigenous residue. **a)** The parameter bulk%mud, you refer to, is a measure applied to the bulk samples. This, in our opinion, makes sense as usually in carbonates, the size fraction < 63 µm is dominated by the periplatform ooze, whereas larger particles mainly comprise pteropod shells and pelagic foraminifers. With this regard, the bulk%mud can be used to trace sea-level variability, as this has been demonstrated by several studies (compare e.g. Boardmann et al., 1986, Droxler et al., 1990; Glaser and Droxler, 1993; Paul et al., 2012; see L278ff). The use of the full grain-size spectrum makes no sense as we talk about organic particles which comprise organisms affected by environmental parameters (neither restricted to nor necessarily affected by sea level) and consequently covering a large size range. Much more important (as stated before) is the relation of shallow-water- vs. pelagic derived organisms– and with this regard, the percentage of particles < 63 µm (bulk%mud) appears to us as a much better measure than the mean grain size. **b)** To our knowledge, there exists no fixed definition for the term "coarse" dust. As stated in L234f, we therefore use this term for Aeolian derived particles in the size range (8-63 µm; i.e. medium to coarse silt). Regarding the term "giant", you're right as this term is commonly used for particles exceeding 63 µm. However, we have not used this term in relation to the data presented in this manuscript but one time with reference to literature where such particles have been described (L404).

11. *My advice is to use an end member model calculate the full range of particles you have in the record. This would give a lot of information and could give answers to several questions which are left open in the current version. Further, if you have, as stated in the Introduction, different wind systems and different source areas you maybe see already a difference in the down core evolution of the single end members. Plus you can calculate log ratios and reconstruct changes in wind speed etc.*

We completely agree that an end-member modeling approach could be promising with regard to grain-size data presented here. This, however, would require comprehensive additional data analyses and more data (and new samples); both beyond the scope of this manuscript. Given this and given that minor revision is requested, we would prefer to leave this for future investigations and for a new manuscript.

12. (L52-74) *It would be very useful to show all these information in an extra figure.*

We have redrawn part of Fig. 1 and the mentioned information has now been included (see also reply to comment 21). An extra figure would contain too much elements which have been already shown in Fig. 1 (map, currents etc.) – this would make no sense in our opinion.

13. (L204-208) *Could be moved to methods section.*

We have moved this paragraph to the grain-size part of the methods section.

14. (L226-229) *Could you include the mean to figure 3?*

Yes, of course. We have now added the mean of the complete grain-size spectrum to Fig. 3 as suggested and to the text where appropriate. However, we still think that the mean is much less meaningful if compared to the d90. This is mainly, because of the predominance of the grain-size fraction < 8 µm, which masks changes in the medium to coarse silt range (compare reply to comment 22).

15. (L231) *How does the distribution look like? Are there several modes existing? I am actually wondering why you are not performing an end member model. The inoculation of the TF90 value etc on an already sieved fraction can easily be incorrect.*

Yes, there are several modes. However, they are restricted to the fraction < 8 µm which is not in the focus of this manuscript. In the medium to coarse silt range there is no distinct "coarse" mode. We do not completely agree to the argument that the d90 could be misleading if calculated on a sieved fraction. This statement is right if we talk of absolute values. But here, where only few to none siliciclastic particles exist in the fraction > 63 µm (which is dominated by carbonate), there will be little difference if compared to the d90 of the full range grain-size spectrum. Furthermore, trends are much more important for this study than absolute values. (for reply to "end-member model" see comment 11)

16. (L234-236) *Do you actually see that in the grain size data, or how were the boundaries decided?*

For the reasons for limiting the investigated grain-size spectrum to 8-63 µm, please see reply to comment 22.

17. (L237) *No data from U1466?*

Available samples from U1466 cover the age range 5-16 Ma, which is beyond the main scope of this paper. Beside this, these samples are affected by early cementation which made them not suitable for grain-size analysis. We therefore decided not to analyze the grain-size distribution but only to include the Sr-Nd data for covering a longer time range with regard to the dust provenance.

18. (L278-279) *...which is very hard, especially when, as you stated in the Introduction, are different source areas and different transport ways involved. You need to isolate the different source areas or transport ways in your record to be able to validate changes within them.*

This comment again focuses on the bulk grain-size data. Please see reply to comment 10b for our explanation on the origin of carbonate bulk sediments.

19. (L323-344) *The difference between fluvial vs. aeolian input and between different sources might be reflected in the grain-size data as well --> end-member modeling.*

Yes, this is potentially valid and there are studies that use end-member models to distinguish between the fluvial and the aeolian component. However, we are not convinced that this approach can be applied to our study area, where fluvial derived material and fine dust falls into comparable grain size ranges… As stated in the reply to point 11 (see above), we agree that end-member modeling is a promising technique and we are curious on the application of this approach to our data, however, this is beyond the scope of this manuscript and must be addressed in a separate study at a later stage.

20. (L419-420) *Why is the fine dust excluded? Could they not be an important piece to the puzzle?*

It is the intention of this study to investigate the (often not considered) medium to coarse dust fraction. Of course, fine dust is an important agent of terrigenous input to the study area (we also mentioned this is the text). However, with regard to the fine dust grain-size range, it is very difficult to distinguish between fluvial and aeolian transported material based on the grain size only (even with end-member modeling). Fine dust contains (and will be mixed with) clay minerals, which are also included in the fluvial derived terrigenous component. This makes it hard to provide solid interpretations with regard to aeolian transport. Furthermore, including the size range of fine dust (< 8 µm) in the grain-size analyses would mask any changes in the medium to coarse dust range as the grain-size spectrum is dominated by clay and fine silt particles.

21. (Fig. 1) *An overview about the broader setting including the different dust source areas and the described wind systems would be helpful.*

We agree to this and have redrawn Fig. 1 accordingly. (see also reply to comment 12)

22. (Fig. 3) *Delete the **sampling dots**, this will make the figure less busy. Why don't you use the **mean grain size**? How is the **8-63 µm** explained?*

Dots: We agree that deleting the dots would make the figure less busy. However, in our opinion, deleting the dots would also remove important information from the figure, e.g. answering the question whether a peak is related to only one sample (outlier?) or supported by several measurements. We therefore intentionally included the dots and prefer to keep them. **Mean grain size:** You are right; the mean is very often used to describe changes in a grain-size distribution. However, in our understanding, changes in the mean of a grain-size distribution are not always related to a real coarsening (or fining) of the complete spectrum – this is only the case if there are no changes in sorting. Regarding the focus of this manuscript, we believe that the d90 is a much more appropriate parameter to trace coarsening and fining of a sample as it is less affected by changes in sorting and provides more reliable information on the size of the largest grains. **8-63 µm:** As explained in the manuscript (L365ff), excluding the clay and fine silt fraction from the grain-size data was necessary to visualize the subtle changes in the medium to coarse silt range which otherwise would have been masked by the majority of grains in the clay to fine silt range. The upper limit (63 µm) has been chosen due to the fact that all samples have been sieved using a 63 µm sieve prior to preparation to

remove the larger carbonate particles (see L158ff). The lower limit (8 µm) is per definition the border between fine and medium silt.

Sebastian Lindhorst
August 2019

Wind variability over the northern Indian Ocean during the past 4 million years – insights from coarse aeolian dust (IODP Exp. 359, Site U1467, Maldives)

Sebastian Lindhorst[1], Christian Betzler[1], Dick Kroon[2]

[1] Universität Hamburg, Zentrum für Erdsystemforschung und Nachhaltigkeit CEN, Institut für Geologie, Bundesstr. 55, 20146 Hamburg, Germany; sebastian.lindhorst@uni-hamburg.de

[2] School of GeoSciences, Grant Institute, University of Edinburgh, The King's Buildings, West Mains Road, Edinburgh EH9 3JW, United Kingdom

Abstract

The lithogenic fraction of carbonate drift sediments from IODP Exp. 359 Site U1467 (Maldives) provides a unique record of atmospheric dust transport over the northern Indian Ocean during the past 4 Myr. Grain-size data provide proxies for dust flux (controlled by source area aridity) as well as wind transport capacity (wind speed). Entrainment and long-range transport of dust in the medium to coarse silt size range is linked to the strength of the Arabian Shamal winds and the occurrence of convective storms which prolong dust transport. Dust flux and the size of dust particles increased between 4.0 and 3.3 Ma, corresponding to the closure of the Indonesian seaway and the intensification of the South Asian Monsoon. There is no clear trend in dust flux between 3.3 and 1.6 Ma, whereas wind transport capacity decreased. Between 1.6 Ma and the Recent, dust flux increased and shows higher variability, especially during the last 500 kyr. Transport capacity increased between 1.2 and 0.5 Ma and slightly decreased since then. Frequency analysis shows that dust transport varies on orbital timescales, with eccentricity control being the most prominent (400 kyr throughout the record, 100 kyr between 2.0 and 1.3 Ma, and since 1.0 Ma). Higher frequency cycles (obliquity and precession) are more pronounced in wind transport capacity than in the amount of dust. This indicates that the amount of coarse dust in sediments from the Maldives as a far-field site is more prone to changes in transport mechanisms than to changes in dust source-area aridity.

Keywords: climate archive, dust, grain size, carbonate drift, South Asian Monsoon, Shamal wind

1. Introduction

Knowledge of the past wind regime over the northern Indian Ocean, so far, comes from the source-proximal Arabian Sea dust records, the isotopic composition of planktonic foraminifera, or is based on data from upwelling areas, where increased productivity is linked to intensified surface winds (Sirocko and Sarnthein, 1989; Kroon et al., 1991; Clemens, 1998; Gupta et al., 2003; 2015). Records of the long-term evolution of the wind field over the northern Indian Ocean are scarce. This study aims to fill this gap by investigating the terrigenous residue of carbonate-drift sediments, which provide an excellent archive of aeolian dust, including the coarse dust fraction, and are unaffected by size sorting effects of oceanic bottom currents (Lindhorst et al., 2019).

Main sources of mineral dust supplied to the western Arabian Sea are the Nubian Desert, the Arabian Peninsula, and desert areas in Iran, Pakistan and Afghanistan as well as in North West India (Middleton, 1986a; Clemens, 1998; Prospero et al., 2002; Léon and Legrand, 2003; Fig. 1). There is an inter-annual latitudinal shift of dust entrainment with low latitudinal sources being active in the winter and higher latitudinal sources becoming more active in late spring and summer (Prospero et al., 2002). Entrainment of dust in Africa and areas located in the inner Arabian Peninsula is largest in spring and summer, whereas in autumn, dust emission is more restricted to the coastal parts of Oman and Somalia (Glennie et al., 2002; Léon and Legrand, 2003). Dust export from the Thar Desert and other areas along the border of Pakistan and India is greatest in summer and autumn (Middleton, 1986a).

Main drivers for dust entrainment in the Arabian Peninsula are the southwest-winds of the summer monsoon and dust-loaded Shamal winds from north-westerly direction (Glennie et al., 2002; Fig. 1). Shamal winds develop along the pressure gradient between the low-pressure monsoon system over India and the high-pressure system over the eastern Mediterranean and are further enhanced by orographic effects along the Persian Gulf (Middleton, 1986b). These winds can override the moist near-surface winds of the southwest monsoon and transport large quantities of dust towards the eastern Arabian Sea, where it is scavenged by summer monsoonal precipitation and wet-deposited (Ackerman and Cox, 1989; Sirocko and Sarnthein,

1989; Yu et al., 2015; Ramaswamy et al., 2017). This process of mid-tropospheric transport also results in a prolonged transport of dust towards the Bay of Bengal and the equatorial Indian Ocean (Ramaswamy et al., 2017; Clemens, 1998). Shamal winds occur in summer as well is in winter, but dust activity is mainly related to the summer Shamal (Yu et al., 2015). Dust transport over the northern Indian Ocean is also prone to the occurrence of tropical cyclones, which can alter the trajectories of dust particles, but can also foster dust entrainment during seasons otherwise characterized by low wind speeds (Ramaswamy, 2014).

In the western Arabian Sea the flux of lithogenic particles is 1.5 to 6 times higher during the southwest (summer-) monsoon (June to September) than during the northeast (winter-) monsoon (December to February), with this gradient being more pronounced in the eastern Arabian Sea (Nair et al., 1989). However, these data did not allow distinguishing aeolian and riverine input and may contain a significant portion of suspended matter supplied by the large rivers draining into the eastern Arabian Sea as this is indicted by radiogenic isotope composition of the sediment that show that the majority of Indus River sediment is deposited in the northern Arabian Sea (Kessarkar et al., 2003).

In this study, a four million year record of aeolian dust transport over the northern Indian Ocean obtained from the terrigenous fraction of carbonate-dominated drift sediments of the Maldives archipelago is presented. Carbonate drifts were deposited in the Maldives Inner Sea, a perched basin, largely isolated from riverine input of coarse material (Kolla et al., 1981; Bunzel et al., 2017; Betzler et al., 2018; Kunkelova et al., 2018).

2. Study site

The Maldives archipelago is an isolated tropical carbonate platform located southwest of India in the northeastern Indian Ocean (Fig. 1). The Maldives carbonate succession accumulated since the Eocene (Aubert and Droxler, 1992; Purdy and Bertram, 1993). Nowadays, the platform is composed of a double row of atolls that enclose a sedimentary basin, the Maldives Inner Sea, which has served as a natural sediment trap of current controlled deposits since the Middle Miocene (Betzler et al., 2017, 2018). Water depths in the Inner Sea are between 300 and 600 m and marine passages, up to several hundreds of metres deep, connect the Inner Sea with the open Indian Ocean, where water depths reach more than 2000 m in the immediate vicinity of the carbonate platform. Due to the bathymetric gradient,

the Maldives Inner Sea represents an isolated perched basin, elevated with regard to the surrounding ocean floor. In consequence, terrigenous input in the Maldives sedimentary record is largely restricted to aeolian transported dust, with a minor component of fluvial derived material delivered by currents from the Arabian Sea and the Bay of Bengal (Kolla et al., 1981). Sedimentation in the Inner Sea is locally controlled by contour currents that accumulate large carbonate drift bodies composed of periplatform ooze around atolls and drowned banks (Betzler et al., 2009, 2013a, 2013b; Lüdmann et al., 2013).

Since around 12.9 Ma, climate and oceanographic setting of the Maldives are controlled by the bi-directional, seasonally reversing South Asian Monsoon system (Wyrtki, 1973; Tomczak and Godfrey, 2003; Betzler et al., 2016). Winds from the southwest prevail during the Northern Hemisphere summer (April to November), whereas northeasterly winds predominate during the winter (November to April). Atmospheric circulation over the Arabian Sea is stronger during the summer monsoon than during the winter monsoon; roughly by a factor of three (Clemens, 1998). Annual precipitation is around 900 mm yr^{-1}; with highest amounts in the summer months (July to September).

The direction of surface ocean currents in the northern Indian Ocean seasonally reverses with the wind system, and are westward-directed in winter and eastward in summer (Shankar et al., 2002). Part of this current system are surface currents that flow along the Indian coast: from the Bay of Bengal to the south-eastern Arabian Sea during winter (West India Coastal Current, WICC; Fig. 1) and vice versa during summer (Shetye, 1998; Shankar et al., 2002; Kurian and Vinayachandran, 2007).

The Maldives are located close to the world's largest sources of dust: North Africa and the Arabian Peninsula providing 58 and 12 wt% of the global dust emissions, respectively (Tanaka and Chiba, 2006). The main input of aeolian dust into the Arabian Sea and towards the northern Indian Ocean is linked to the prevailing southwest winds during the summer monsoon and subordinated north-westerly Shamal winds (Clemens, 1998; Ackerman and Cox, 1989; Nair et al., 1989; Prospero et al., 2002; Yu et al., 2015; Ramaswamy et al., 2017; Banerjee et al., 2019). These winds entrain dust from the arid areas in northeast Africa and the Arabian Peninsula, which is subsequently scavenged by monsoonal rains into the ocean. By contrast, satellite based measurements on the aerosol optical thickness show that the modern dust plume of the winter monsoon clearly reaches the Maldives (Kunkelova et al., 2018). Measurements at the Maldives Climate Observatory at Hanimaadhoo Atoll in the northern Maldives and numerical models of the seasonality of aerosol loadings in south Asia underline

this seasonality in the composition and provenance of aerosols: highest concentrations of (coarse) mineral dust from April to September, whereas fine dust including sulphate and black carbon of anthropogenic origin reach peak concentrations from November to January with the portion of coarse minerogenic dust being by far lower than during the rest of the year (Eck et al., 2001; Chowdhury et al., 2001; Stone et al., 2007; Adhikary et al., 2007; Das et al., 2011).

IODP (Integrated Ocean Drilling Program) site U1467 (4°51.0274′N, 73°17.0223′E, water depth 487.4 m) was drilled during Expedition 359 in October 2015. Site U1467 recovered a 630 m thick sequence of pelagic carbonate drift deposits from the eastern Inner Sea of the Maldives and provides a well-preserved, continuous record of lithogenic input into the south-eastern Arabian Sea (Betzler et al., 2017; Kunkoleva et al., 2018).

3. Methods

Sampling of IODP Exp. 359 Site U1467 cores was done in April and May 2016 under the sample request 29856IODP. Sampling followed the shipboard splice information (splice-359-U1467-BCD-20160114; IODP LIMS Database: http://iodp.tamu.edu/database/) and comprised samples of 10 cm^3 each. All depth readings in this work refer to the depth scale CCSF-359-U1467-ABCD-20160114) and are given in metres of composite depth (mcd).

3.1 Grain-size analysis and statistics

Samples for bulk grain size were wet sieved (2000 µm) prior to measurement to remove very coarse particles like coral detritus and large pteropod shells. Samples for the determination of the terrigenous grain-size spectrum were wet sieved using a 63 µm sieve to remove the larger carbonate particles. Chemical treatment followed the workflow described by McCave et al. (1995): the bulk fraction < 63 µm was heated in H_2O_2 to oxidize the organic portion, and subsequently treated with 1M Ca_3COOH (acetic acid) to dissolve the carbonate. Biogenic opal was removed with 2M $NaHCO_3$ (sodium bicarbonate). Samples of the terrigenous residue were visually inspected by means of a binocular microscope to ensure complete dissolution of carbonate and biogenic silica as well as complete disintegration of aggregates. Prior to grain-size measurement, all samples were dispersed in water using

ultrasonic and 0.05% $Na_4P_2O_7$ x 10 H_2O (tetra-sodium diphosphate decahydrate) as dispersing agent. Measurements were done using a Sympatec Helos KFMagic laser particle-size analyser and measuring ranges of 0.5/18-3500 µm for bulk grain size and 0.25-87.5 µm for the non-carbonate residual, respectively. To ensure accuracy of measurements and absence of a long-term instrumental drift, an in-house grain-size standard was measured daily prior to the series of measurements (standard deviation was <0.1 µm for the measuring range 0.25-87.5 µm and <3.3 µm for 0.5/18-3500 µm, respectively).

Grain-size statistics are based on the graphical method (Folk and Ward, 1957) and were calculated using Gradistat (Blott and Pye, 2001). Values for percentages are rounded to the nearest integer. Correlation coefficients are based on the Spearman rank correlation, as this method supports nonlinear correlations.

Below 174.34 mcd (metres core depth) deposits at IODP Exp. Site U1467 show chert concretions. These aggregates could not be disintegrated by means of chemical treatment and as a consequence caused an apparent coarsening of the grain-size spectrum. All grain-size data from below 174.10 mcd (corresponding to a depositional age of 4.0 Ma) are therefore excluded from further interpretation.

3.2 Age model

The initial age framework for Site U1467 samples is based on biostratigraphic (calcareous nannofossils and planktonic foraminifera) and magnetostratigraphic data as provided by Betzler et al. (2017). The early Pliocene part of the biostratigraphic age model (from 3.1 Ma) is in good agreement with magnetic stratigraphic data from the same site (Lanci et al., this volume). The long-term averaged sedimentation rate is 3.4 cm kyr^{-1} for the last 4 Myr (Betzler et al., 2017). This does not take into account that periplatform carbonates show variable sedimentation rates reflecting the flooding or emersion of the banks and atolls surrounding the Inner Sea and consequently the export of shallow-water material from these areas. This effect is especially pronounced with the inception of the high amplitude sea-level variations for the past 0.75 Myr after the Mid-Pleistocene Transition (MPT). To overcome this shortcoming, we correlate the bulk grain-size data of Site U1467 with the sea-level data of Miller et al. (2005) and the global oxygen isotope stack LR04 (Lisiecki and Raymo, 2004): finer grained periplatform ooze forms during sea-level highstand when the platforms export large amount of carbonate (Boardmann et al., 1986, Glaser and Droxler, 1993). For the Maldives, the validity of this assumption has been shown by Paul et al. (2012) and Bunzel et al. (2017).

Correlation was done by manual correlation of minima in bulk grain size and sea-level lows. Subsequently, local highs in sea level were linked with corresponding fine peaks in bulk grain size.

Correlations and all time-depth conversions were done using Analyseries 2.0.8 (Paillard et al., 1996). Wavelet spectra were calculated with PAST (Hammer et al., 2001), same for insolation data, where the algorithms of Laskar et al. (2004) and the data of Huybers and Eisenman, (2006) have been used. Sample size for wavelet spectra is 0.007 Myr.

4. Results

4.1 Age model

The final age model for Site U1467 samples accounts for the carbonate-productivity controlled variability of the sedimentation rate on orbital time scales. Sedimentation rates for Site U1467 are 1.0 to 26.5 cm kyr^{-1}, with a median of 3.8 cm kyr^{-1} (Fig. 2). In general, sedimentation rates are higher and less variable in the older part of the record, compared to the youngest part: sedimentation rates of 1.6 to 9.3 cm kyr^{-1} (median 5.9 cm kyr^{-1}) between 4.0 to 3.0 Ma contrast with rates of 1.0 to 26.5 cm kyr^{-1} (median 4.7 cm kyr^{-1}) between 1.0 Ma and the Recent.

4.2 Grain-size distribution

Sample recovery and using our age model resulted in time-variable sample intervals of 0.0009-0.039 Myr (median 0.0053 Myr) and 0.0009-0.0778 Myr (median 0.0055 Myr) for bulk grain size and terrigenous residue, respectively. Each sample (thickness c. 1.5 cm) represents the integrated sedimentation over a period of 290 yrs (range 57 to 1,500 yrs), on average.

The portion of mud-size particles (< 63 µm; $Bulk_{\%Mud}$) varies between 28 and 100 % of the bulk fraction with a median of 77 % (Fig. 3). The highest mud contents (> 95 %) are in the oldest part of the record (4.0-3.6 Ma) and around 2.0 Ma; lowest mud contents occur between 2.4-2.1 and around 1.0 Ma. There is an overall coarsening of the bulk fraction starting at 4.0 Ma until reaching the absolute minimum in $Bulk_{\%Mud}$ around 2.3 Ma, which is followed by a rapid fining until 2.0 Ma. $Bulk_{\%Mud}$ stays around 80 % until 1.05 Ma, where an abrupt

224 coarsening starts. Subsequently, and until the Recent, there is an overall fining, superimposed
225 by pronounced higher frequency changes with amplitudes of 20 % and greater.

226 The grain size of the terrigenous fraction is characterized by the 90th percentile of the
227 grain-size spectrum < 63 µm (TF_{d90}) and the percentage of particles in the grain-size range 8
228 to 63 µm ($TF_{\%8-63}$). TF_{d90} serves as a measure for the coarsest particles in this size range and,
229 with respect to dust, provides information on wind transport capacity (i.e. wind speed). In
230 addition, $TF_{\%8-63}$ is regarded as a proxy for the total amount of dust in the medium to coarse
231 silt range (here referred to as coarse dust). The mean grain size of the terrigenous fraction <63
232 µm is provided for comparison (Fig. 3).

233 At Site U1467, $TF_{\%8-63}$ ranges from 28 to 68 %, with a median of 48 %. Lowest
234 percentages are present prior to 3.6 Ma and highest values occur around 3.3 Ma and in the
235 youngest part of the record, i.e. the past 0.6 Myr. There is an overall coarsening of the
236 terrigenous fraction throughout the record, and with respect to long-term trends, different
237 periods can be distinguished: A coarsening from 4.0 to 3.3 Ma is followed by a rapid decrease
238 of the amount of coarse dust until 3.1 Ma. Between 3.1 and 2.4 Ma, there is no clear trend.
239 Subsequently, until 1.8 Ma, $TF_{\%8-63}$ increases, before it reaches a minimum around 1.6 Ma.
240 Afterwards, there is a coarsening until 0.6 Ma. The youngest period, 0.6 Ma to the Recent is
241 characterized by a high variability of the amount of coarse particles.

242 The mean grain size of the terrigenous fraction <63 µm ($TF_{Mean\ <63}$) varies between 2.7
243 and 8 µm (median 3.8 µm); the size of the coarsest particles in the terrigenous fraction (TF_{d90})
244 ranges from 9.4 to 21.4 µm (median 13.4 µm). TF_{d90} is finest prior to 3.8 Ma and coarsest
245 around 3.3 Ma. With regard to long-term trends, three intervals can be distinguished: first, a
246 coarsening until 3.3 Ma, followed by, second, an overall fining until 1.6 Ma, and subsequently
247 a coarsening of TF_{d90} until today.

248 Visually, the curves of $TF_{\%8-63}$ and TF_{d90} appear to have a similar shape. The
249 mathematical correlation of both curves, however, is only 0.6 ($p < 0.0001$) and long-term
250 trends are slightly different. $TF_{\%8-63}$ and TF_{d90} both show a coarsening from 4.0 to 3.3 Ma.
251 Subsequently, the size of the coarsest particles slightly decreases until 1.2 Ma, whereas their
252 percentage remains stable until 1.6 Ma. The overall coarsening in the younger part of the
253 record starts around 1.6 Ma if $TF_{\%8-63}$ is considered, and later, at 1.2 Ma, if the absolute size
254 of the largest particles (TF_{d90}) is taken as a measure.

255 The wavelet spectra of both, $TF_{\%8-63}$ and TF_{d90}, show the presence of cyclic variability on
256 orbital timescales (Fig. 4). Frequencies in the precessional (23 kyr) and the obliquity (41 kyr)

band are more pronounced in the size of the coarsest particles (TF_{d90}), than in the percentage of coarse particles ($TF_{\%8-63}$). The short eccentricity cycle (100 kyr) is present in both grain-size parameters after 2.0 Ma, but weakens between 1.6 and 1.0 Ma ($TF_{\%8-63}$) and 1.3 and 1.0 Ma (TF_{d90}), respectively. The influence of the short eccentricity cycle is also weak in the older part of the record. The long eccentricity cycle with a frequency of around 400 kyr is present in both datasets, but weak prior to 2.0 Ma in the $TF_{\%8-63}$ record, whereas it persists throughout the record in the TF_{d90} data.

5. Discussion

5.1 Bulk sediment grain size

Site U1467 has been cored in carbonate drifts consisting of periplatform ooze formed through off-bank transport of carbonate particles from the shallow water carbonate factories and pelagic carbonate- and silica production. We interpret the bulk grain-size data to reflect varying input from these sources. In general, a fining of carbonate drift sediments is expected during sea-level highstands, when export of mud-size particles from shallow-water banks and atolls is at its maximum (Boardmann et al., 1986, Droxler et al., 1990; Glaser and Droxler, 1993; Paul et al., 2012). Coarsening, by contrast, occurs when sea level is low and banks and atolls emerge. In addition to this higher frequency variability interpreted to be triggered by sea-level, there are long-term trends in the bulk grain size from Site U1467 that do not correlate with published sea-level records (Fig. 3). The origin of these changes in bulk grain size has to remain speculative until a detailed analysis of the components is available. Such data would not only allow quantifying shallow-water and pelagic origin of carbonate particles, but also detecting changes in the water masses that bath the carbonate platform.

5.2 Glacial-interglacial variability and provenance of coarse dust

Studies on the dust records of the Arabian Sea and elsewhere have shown that lithogenic grain size is a reliable measure for wind transport capacity (i.e. wind speed), whereas the amount of dust, as indicated by lithogenic mass accumulation rates and the percentage of the lithogenic component, is controlled by source area aridity rather than transport energy (Prell and van Campo, 1986; Tsoar and Pye, 1987; Clemens and Prell, 1990; Clemens et al., 1991).

288 This study focuses on aeolian transported dust in the medium to coarse silt range (coarse
289 dust). The grain-size distribution of the terrigenous residue is characterized by i) the size of
290 the 90th percentile of the size range 8-63 µm (TF_{d90}) as a measure for the largest particles, and
291 ii) the percentage of particles in the size range 8-63 µm ($TF_{\%8-63}$) in relation to the total
292 amount of terrigenous particles < 63 µm. The clay and fine silt fraction (< 8 µm) has been
293 excluded to avoid bias due to the presence of the clay and fine dust particles which potentially
294 would mask subtle changes in the medium to coarse silt fraction (Lindhorst et al., 2019). This
295 dominance of the fine particles is illustrated by the comparable little variability in the mean
296 grain size of the particle spectrum < 63 µm (Fig. 3).

297 The variability of the lithogenic component of Maldivian carbonate drift sediments, as
298 recorded by element ratios derived by means of x-ray fluorescence (XRF) core scanning, has
299 been previously linked to precipitation changes in the dust source areas which are controlled
300 by the monsoonal system (Bunzel et al., 2017; Kunkelova et al., 2018). During glacial
301 periods, reduced precipitation and the intensification of the winter monsoon winds (from the
302 NE) causes increased mechanical weathering in the source areas and leads to higher dust flux
303 rates. Interglacial periods, by contrast, are characterized by more humid conditions due to a
304 stronger summer monsoon (winds from the SW), which results in higher continental discharge
305 rates, the intensification of chemical weathering, and increased input of fluvial material into
306 the ocean, whereas aeolian dust flux is expected to be reduced. Same is valid for the western
307 Arabian Sea, where dust flux as indicated by mass accumulation rates positively correlates
308 with global ice volume and as such is increased during glacial times (Clemens and Prell,
309 1990). Dust particle size, a measure for transport capacity, by contrast, varies on shorter time
310 scales and appears to be decoupled from dust flux (Clemens and Prell, 1990). Such a
311 decoupling of dust flux and transport capacity has also been observed in trans-Atlantic dust
312 transport, where it is interpreted to reflect the variability of different transport mechanisms
313 responsible for fine and coarse dust transport, respectively (Lindhorst et al., 2019).

314 Comparison of the Arabian Sea dust records and the XRF-based data from the Maldives,
315 with the grain-size data of the coarse dust fraction of Site U1467 presented in this study
316 reveals a different picture. During glacial periods, the total amount of dust, as traced by the
317 percentage of particles falling into the 8-63 µm size range, decreases and particles are finer
318 (smaller TF_{d90}) compared to samples from interglacial times (Fig. 3). This pattern, however, is
319 persistent only during the middle and late Pleistocene, from about 0.9 Ma until the Recent,
320 whereas there is no such clear relation in older parts of the record.

There are different possibilities to explain the observed negative correlation on glacial to interglacial time scales between the coarse dust data from Site U1467 and published dust records from the Arabian Sea. First, dust transport paths, controlled by the wind regime over the northern Indian Ocean are different during glacial times in reaction to altered northern hemisphere temperature gradients and precipitation patterns. This would potentially allow less dust to reach the Maldives. Second, the transport mechanisms responsible for the transport of coarse dust could be weaker during glacials. Beside dust entrainment, such mechanisms must ensure the continuous re-suspension of larger particles to avoid gravitational settling and to prolong transport distances. Coarse dust transport over the Arabian Sea has been shown to be linked with the strength of north-westerly Shamal winds (Sirocko and Sarnthein, 1989; Clemens, 1998; Ackerman and Cox, 1989; Nair et al., 1989; Glennie et al., 2002; Ramaswamy et al., 2017; Banerjee et al., 2019). In the Atlantic, the transport of coarse and giant African dust particles as far as the Caribbean Sea has been proposed to be linked to the occurrence of convective storm systems, which ensure deep atmospheric convection of dust particles and ensures prolonged transport (Prospero et al., 1970; Betzer et al. 1988; van der Does et al., 2018; Lindhorst et al., 2019). Similar mechanisms are imaginable for the transport of coarse dust to the Maldives, roughly 3000 km away from the potential dust sources in northeast Africa and the Arabian Peninsula. Less frequent occurrence of convective storms during glacial times, potentially as the result of lower sea-surface temperatures, would result in the observed fining of the coarse dust from Site U1467.

The negative correlation of the geochemical dust records from the Maldives (Bunzel et al., 2017; Kunkelova et al., 2018) and the coarse dust record as presented in this study is seen to result from different particle-size ranges: Element ratios were measured by XRF scanning of complete cores and as such are expected to be dominated by the mud fraction of the sediments, especially clay minerals and fine dust particles. Grain-size data of the terrigenous residue as presented in this study, by contrast, only incorporate particles in the size range 8 to 63 µm and does not take into account finer dust particles. Fine dust particles are nowadays enriched in north-easterly winter monsoonal winds (Eck et al., 2001; Chowdhury et al., 2001; Stone et al., 2007; Adhikary et al., 2007; Das et al., 2011). In addition, the West India Coastal Current (WICC), transports large water- and suspended sediment masses from the Bay of Bengal into the south-eastern Arabian Sea during the winter monsoon (Shetye, 1998; Shankar et al., 2002; Kurian and Vinayachandran, 2007; Fig. 1). Bulk terrigenous records, dominated by particles in the clay and fine silt range, are therefore prone to changes in the winter monsoon. Coarse dust particles, by contrast, are predominantly deposited during the summer

355 monsoon and periods of north-westerly Shamal winds (Clemens, 1998; Ramaswamy et al.,
356 2017; Banerjee et al., 2019). These particles are therefore expected to originate most likely
357 from dust source areas towards the west and northwest, namely northeast Africa and the
358 Arabian Peninsula.

359 To summarize, grain-size data of the terrigenous medium to coarse silt fraction (8-63 µm)
360 of Site U1467 sediments are interpreted to reflect i) the amount of transported coarse dust as
361 controlled by source area aridity and/or transport paths; and ii) the dust transport capacity as
362 controlled by the transport mechanisms, i.e. wind intensity of the Shamal wind system and/or
363 occurrence of convective storm systems. Based on the data available, a particle-size
364 dependent source is proposed for the terrigenous material deposited in the Maldives carbonate
365 drifts. Particles in the clay and fine silt range derive from rivers draining into the Bay of
366 Bengal, from where they are transported westward by the WICC during the winter monsoon.
367 By contrast, coarse dust particles likely originate from dust sources in northeast Africa and the
368 Arabian Peninsula. For these particles, a mid-tropospheric transport is proposed, initiated by
369 the north-westerly winds of the Shamal wind system which override the south-westerly winds
370 of the summer monsoon (Clemens, 1998; Ackerman and Cox, 1989; Nair et al., 1989;
371 Ramaswamy et al., 2017; Banerjee et al., 2019). As such, the grain-size data from IODP Site
372 U1467 are seen to record the variability in coarse-dust transport during the summer monsoon,
373 whereas geochemical records from the same site reflect the variability of fine particle input by
374 winter monsoonal winds and riverine input from the Bay of Bengal.

375 The proposed particle-size dependence of dust provenance has also implications for the
376 study of dust source areas based on radiogenic isotopes, like e.g. strontium and neodymium
377 isotope ratios, which are established proxies for terrigenous sediment provenance, including
378 marine sediments from the Indian Ocean (Goldstein and Jacobsen, 1987; Colin et al., 1999;
379 Jung et al., 2004; Ahmad et al., 2005; Goswami et al., 2012; Sharifi et al., 2018). Strontium
380 and neodymium isotope ratios address the provenance of bulk terrigenous material. In the fine
381 fraction the isotopic signal is due to the host minerals of Sr and Nd (zircon, monazite/allanite,
382 clay minerals, titanite and biotite), which are in the clay- to silt-sized fraction of the sediment
383 (Innocent et al., 2000; Meyer et al., 2011). Aeolian sediment provenances based on bulk-
384 terrigenous isotope ratios therefore has to be treated with caution as fine and coarse dust do
385 not necessarily originate from the same sources nor follow the same transport paths.

386

387 **5.3 Four million years of dust transport over the northern Indian Ocean**

388 Grain-size data from the terrigenous residue of Site U1467 sediments provide a four
389 million year record of coarse dust transport over the northern Indian Ocean, a key area for the
390 understanding of long-term changes in the South Asian wind systems.

391 The amount of coarse dust that reached the Maldives Inner Sea increased on the long-term
392 since 4 Myr ago ($TF_{\%8-63}$; Fig. 3). The strongest increase occurred between 4.0 to 3.3 Ma.
393 Dust transport capacity, as mirrored by the size of the largest dust particles (TF_{d90}), increased
394 at the beginning of the record, between 4.0 to 3.3 Ma, as such paralleling the increase in the
395 amount of coarse dust. In addition, the coarsest particles of the record, indicating highest
396 transport intensities during the last 4 Myr, are found around 3.3 Ma.

397 Both, the increase in dust flux as well as of transport capacity are synchronous with the
398 closure of the Indonesian seaway (4 to 3 Ma) and the resulting long-term cooling of ocean
399 surface waters in the Indian Ocean (Rodgers et al., 2000; Cane and Molnar, 2001). The
400 resulting reorganization in ocean- and atmospheric circulation is assumed to be the trigger of
401 the late Pliocene aridification in northeast Africa and other circum-North Indian Ocean dust
402 source areas, as well as occurred synchronous to the intensification of the South Asian
403 Monsoon (Cane and Molnar, 2001; Zhang et al., 2009; Sun et al., 2010; Anderson et al.,
404 2019). Both processes could have increased dust flux to the Maldives on the long-term.

405 From 3.3 to around 3.1 Ma grain-size data show a rapid decrease in dust flux and transport
406 capacity. This event occurs simultaneously to the mid-Pliocene warm period; a time
407 characterized by sea-surface temperatures 2.7 to 4 °C higher than today (mPWP; 3.3-3.0 Ma;
408 Haywood et al., 2016). Higher sea-surface temperatures are likely to have increased
409 precipitation in the dust source regions (Goddard and Graham, 1999; Rodgers et al., 2000),
410 resulting in less dust export. However, the coarsening of TF_{d90} between 3.1 and 3.0 Ma and
411 the elevated values for dust flux at the same time, indicate that dust transport over the
412 northern Indian Ocean was not uniformly reduced during the mPWP.

413 Between 3.0 and 1.6 Ma, dust transport capacity is variable but decreases over the long-
414 term. Dust flux at the same time shows no clear trend, but a temporary increase between 2.2
415 and 1.8 Ma. The global climate past 3.0 Ma is characterized by northern hemisphere cooling
416 and the onset of extended glaciations (starting around 2.7 Ma, Shackleton et al., 1984; Haug et
417 al., 1999). More locally, in the Indian Ocean dust source regions, the long-term aridification,
418 which started around 4.0 Ma, intensified as indicated by numerous records from east Africa,
419 where former forest and grassland areas diminished during this period (deMenocal, 1995,
420 2004, 2005; Cane and Molnar, 2001; Sun et al., 2010; Nie, 2017). With regard to coarse dust,

these changes in vegetation would corroborate the observed overall increase in dust flux during the last 2.4 Myr. By contrast, Arabian Sea and northern Indian Ocean wind systems, as mirrored by dust transport capacity, show no clear trend during this time. This underlines the role of source area aridity for dust flux, and as such points to a decoupling of dust flux rate from the size of transported dust particles, as described from dust records elsewhere (Clemens and Prell, 1990; Lindhorst et al., 2019).

During the last 1.6 Myr there is an increase in dust flux again, whereas transport capacity remained at a low level until the onset of the mid-Pleistocene transition (MPT; 1.25-0.75 Ma; Clark et al., 2006). During the MPT, there is no clear trend in both dust records from Site U1467. However, with the onset of the pronounced Pleistocene glacial-interglacial variability, past 0.9 Ma, the amplitude of changes in both, dust flux and dust transport capacity, increased paired with elevated dust flux rates and a coarsening of the dust grain-size spectrum. In the late Quaternary, since around 500 ka, peak dust-flux rates are higher than during any other time in the last 4 Myr.

5.4 Cyclic variability of dust transport

The visual inspection of the terrigenous grain-size data implies periodic changes of dust flux rate and dust transport capacity (Fig. 3). This is supported by wavelet spectra, which show a cyclic variability of $TF_{\%8\text{-}63}$ and TF_{d90} on orbital timescales (Fig. 4).

Higher frequency orbital-driven cycles in the precessional (23 kyr) and the obliquity (41 kyr) band are more pronounced in the variability of the particle size (TF_{d90}), than in the percentage of coarse particles ($TF_{\%8\text{-}63}$), indicating that the dust transport mechanisms (wind systems) are more prone to higher frequency orbital-driven climatic changes than the total dust flux, which is controlled by long-term changes of source-area precipitation. This interpretation stands in line with previous studies, which showed the prevalence of precessional and obliquity controlled variability in summer insolation on the strength of the South Asian Monsoon system, whereas dust flux rates are dominated by the longer periodicity of glacial-interglacial climate changes, suggesting a link to high-latitude climate variability (deMenocal, 1995; Clemens et al., 1996; Clemens, 1998; Sun et al., 2010; Bunzel et al., 2017; Nie, 2017). This, however, stands in contrast to a very recent study, which suggests that dust flux from the Sahara rather follows a precessional variability than changes on glacial-interglacial timescales (Skonieczny et al., 2019).

453 Low-frequency orbital-driven cyclicities in the Site U1467 dust records encompass the
454 two eccentricity cycles with wavelengths of 100 and c. 400 kyr. The short eccentricity cycle is
455 present in both grain-size records past 2.0 Ma, whereas it remains speculative beforehand.
456 The influence of the short eccentricity weakens between 1.6 and 1.0 Ma (dust flux) and 1.3
457 and 1.0 Ma (transport capacity), respectively. The long eccentricity cycle seems to influence
458 both, dust flux rate and transport capacity. However its influence on the dust flux rate is weak
459 prior to 2.0 Ma, whereas it persists throughout the record if only transport capacity is
460 considered.

461

462 ## 6. Conclusions

463

464 Carbonate drift sediments at IODP Site U1467 from the Maldives Inner Sea provide an
465 archive of coarse dust transport over the northern Indian Ocean during the last 4 million years.
466 Based on grain-size data of the terrigenous residue, variability in dust flux and wind transport
467 capacity has been reconstructed. Dust flux and wind transport capacity increased between 4.0
468 and 3.3 Ma, as such paralleling the closure of the Indonesian seaway and the resulting
469 reorganization of the wind- and precipitation regime of the western Indian Ocean. In this
470 context, the increase in grain size is interpreted to indicate an intensification of transport
471 capacity, i.e. higher wind speeds in the north-westerly Shamal winds and/or more frequent
472 convective storms, whereas the increase in dust flux points to more arid conditions in the dust
473 source areas, primarily in northeast Africa and the Arabian Peninsula. Subsequently, there is
474 variability but no clear trend in dust flux between 3.3 and 1.6 Ma, whereas transport capacity
475 decreased during this period. Between 1.6 and the Recent, dust flux increased and shows
476 higher variability, especially since 500 ka. Transport capacity reached a low around 1.2 Ma
477 and increased until 500 ka. Since then, transport capacity slightly decreased.

478 Frequency analysis shows that coarse dust transport varies on orbital timescales, with the
479 eccentricity control being the most prominent. Higher frequencies, as the result of changes in
480 obliquity and precession, are more pronounced in the record of wind transport capacity than in
481 the amount of coarse dust. This indicates that the transport of coarse dust to the Maldives as a
482 far field site is more prone to changes in mechanisms (i.e. intensity of the Shamal winds,
483 occurrence of convective storm systems, direction of transport) than to environmental changes
484 in the dust source areas (precipitation rates, vegetation coverage).

485

486 Acknowledgements

487 The authors would like to thank the International Ocean Discovery Programm (IODP) for
488 providing samples and data and the crew, scientific staff and shipboard science party of Joides
489 Resolution for making Exp. 359 possible. Jutta Richarz (University of Hamburg) is thanked
490 for chemical sample treatment and grain-size measurements, and Max Bohlen, Catalina
491 Vulpe, and Anna-Lena Geßner for sample preparation. Liviu Giosan (Woods Hole
492 Oceanographic Institution) is thanked for discussions on sediment provenance and radiogenic
493 isotopes. The manuscript has been significantly improved by the detailed and thorough
494 reviews made by two anonymous reviewers.

495

496 Data availability

497 Grain-size statistics for samples from Site U1467 are available from the data depository
498 PANGAEA: doi: XXX (*will be added once available*). For grain-size parameters presented in
499 this manuscript see supplementary material.

500

501 REFERENCES

502 Ackerman, S.A. and Cox, S.K., 1989. Surface weather observations of atmospheric dust over
503 the southwest summer monsoon region. Meteorology and Atmospheric Physics, 41, 19-34.

504 Adhikary,B., Carmichael,G.R., Tang,Y., Leung,L.R., Qian,Y., Schauer,J.J., Stone,E.A.,
505 Ramanathan,V., Ramana,M.V., 2007. Characterization of the seasonal cycle of south Asian
506 aerosols: A regional-scale modelling analysis. Journal of Geophysical Research, 112,
507 D22S22.

508 Ahmad, S.M., Anil Babu, G., Padmakumari, V.M., Dayal, A.M., Sukhija, B.S.,
509 Nagabhushanam, P., 2005. Sr, Nd isotopic evidence of terrigenous flux variations in the Bay
510 of Bengal: Implications of monsoons during the last ~34,000 years. Geophysical Research
511 Letters 32, 1-4.

512 Anderson, C.H., Murray, R.W., Dunlea, A.G., Giosan, L., Kinsley, C.W., McGee, D., Tada,
513 R., 2019. Aeolian delivery to Ulleung Basin, Korea (Japan Sea), during development of the

East Asian Monsoon through the last 12 Ma. Geological Magazine, doi.org/10.1017/S001675681900013X.

Aubert, O. and Droxler, A.W., 1992. General Cenozoic evolution of the Mal-dives carbonate system (equatorial Indian Ocean). Bulletin des Centres de Recherches Exploration-Production Elf-Aquitaine, 16, 113-136.

Banerjee, P., Satheesh, S.K., Moorthy, K.K., Nanjundiah, R.S., Nair, V.S., 2019. Long-range transport of mineral dust to the northeast Indian Ocean: Regional versus remote sources and the implications. Journal of Climate, 32, 1525-1549.

Betzer, P.R., Carder, K.L., Duce, R.A., Merrill, J.T., Tindale, N.W., Uematsu, M., Costello, D.K., Young, R.W., Feely, R.A., Breland, J.A., Bernstein, R.E., Greco, A.M., 1988. Long-range transport of giant mineral aerosol-particles. Nature, 336, 568-571.

Betzler, C., Hübscher, C., Lindhorst, S., Reijmer, J.J.G., Römer, M., Droxler, A.W., Fürstenau, J., and Lüdmann, T., 2009. Monsoon-induced partial carbonate platform drowning (Maldives, Indian Ocean). Geology, 37, 867-870.

Betzler, C., Fürstenau, J., Lüdmann, T., Hübscher, C., Lindhorst, S., Paul, A., Reijmer, J.J.G., and Droxler, A.W., 2013a. Sea-level and ocean-current control on carbonate-platform growth, Maldives, Indian Ocean. Basin Research, 25, 172-196.

Betzler, C., Lüdmann, T., Hübscher, C., and Fürstenau, J., 2013b. Current and sea-level signals in periplatform ooze (Neogene, Maldives, Indian Ocean). Sedimentary Geology, 290, 126-137.

Betzler, C., Eberli, G.P., Kroon, D., Wright, J.D., Swart, P.K., Nath, B.N., Alvarez-Zarikian, C.A., Alonso-Garciá, M., Bialik, O.M., Blättler, C.L., Guo, J.A., Haffen, S., Horozal, S., Inoue, M., Jovane, L., Lanci, L., Laya, J.C., Mee, A.L.H., Lüdmann, T., Nakakuni, M., Niino, K., Petruny, L.M., Pratiwi, S.D., Reijmer, J.J.G., Reolid, J., Slagle, A.L., Sloss, C.R., Su, X., Yao, Z., Young, J.R., 2016. The abrupt onset of the modern South Asian Monsoon winds. Scientific Reports 6, 1-10.

Betzler, C., Eberli, G., Alvarez Zarikian, C., Alonso-García, M., Bialik, O., Blättler, C., Guo, J., Haffen, S., Horozal, S., Inoue, M., Jovane, L., Kroon, D., Lanci, L., Laya, J., Ling Hui Mee, A., Lüdmann, T., Nakakuni, M., Nath, B., Niino, K., Petruny, L., Pratiwi, S., Reijmer, J., Reolid, J., Slagle, A., Sloss, C., Su, X., Swart, P., Wright, J., Yao, Z., Young, J., 2017. Expedition 359 summary. Proceedings of the International Ocean Discovery Program. doi: 10.14379/iodp.proc.359.101.2017.

546 Betzler, C., Eberli, G.P., Lüdmann, T., Reolid, J., Kroon, D., Reijmer, J.J.G., Swart, P.K.,
547 Wright, J., Young, J.R., Alvarez-Zarikian, C., Alonso-García, M., Bialik, O.M., Blättler, C.L.,
548 Guo, J.A., Haffen, S., Horozal, S., Inoue, M., Jovane, L., Lanci, L., Laya, J.C., Hui Mee, A.L.,
549 Nakakuni, M., Nath, B.N., Niino, K., Petruny, L.M., Pratiwi, S.D., Slagle, A.L., Sloss, C.R.,
550 Su, X., Yao, Z., 2018. Refinement of Miocene sea level and monsoon events from the
551 sedimentary archive of the Maldives (Indian Ocean). Progress in Earth and Planetary Science
552 5, 1-18.

553 Blott, S.J. and Pye, K., 2001. GRADISTAT: a grain size distribution and statistics package
554 for the analysis of unconsolidated sediments. Earth Surface Processes and Landforms, 26,
555 1237-1248.

556 Boardman, M. R., Neumann, A. C., Baker, P. A., Dulin, L. A., Kenter, R. J., Hunter, G. E.,
557 Kiefer, K. B., 1986, Banktop responses to Quaternary fluctuations in sea level recorded in
558 periplatform sediments Geology, 14, 28-31.

559 Bunzel, D., Schmiedl, G., Lindhorst, S., Mackensen, A., Reolid, J., Romahn, S., Betzler, C.,
560 2017. A multi-proxy analysis of Late Quaternary ocean and climate variability for the
561 Maldives, Inner Sea. Climate of the Past, 13, 1791-1813.

562 Cane, M.A. and Molnar, P., 2001. Closing of the Indonesian seaway as a precursor to east
563 African aridification around 3-4 million years ago. Nature, 411, 157-162.

564 Chowdhury, Z., Hughes, L.S., Salmon, L.G., 2001. Atmospheric particle size and
565 composition measurements to support light extinction calculations over the Indian Ocean.
566 Journal of Geophysical Research, 106, D22, 28597-28605.

567 Clark, P.U., Archer, D., Pollard, D., Blum, J.D., Rial, J.A., Brovkin, V., Mix, A.C., Pisias,
568 N.G., Roy, M., 2006. The middle Pleistocene transition: characteristics, mechanisms, and
569 implications for long-term changes in atmospheric pCO2. Quaternary Science Reviews, 25,
570 3150-3184.

571 Clemens, S.C. and Prell, W.L., 1990. Late Pleistocene variability of Arabian Sea summer
572 monsoon winds and continental aridity: eolian records from the lithogenic component of
573 deep-sea sediments. Paleoceanography, 5, 109-145.

574 Clemens, S., Prell, W., Murray, D., Shimmield, G., Weedon, G., 1991. Forcing mechanisms
575 of the Indian Ocean monsoon. Nature, 353, 720-725.

576 Clemens, S.C.,Murray, D.W., Prell, W.L., 1996. Nonstationary Phase of the Plio-Pleistocene
577 Asian Monsoon. Science, 274, 943-948.

578 Clemens, S.C., 1998. Dust response to seasonal atmospheric forcing: Proxy evaluation and
579 calibration. Paleoceanography, 13, 471-490.

580 Colin, C., Turpin, L., Bertaux, J., Desprairies, A., Kissel, C., 1999. Erosional history of the
581 Himalayan and Burman ranges during the last two glacial-interglacial cycles. Earth and
582 Planetary Science Letters 171, 647-660.

583 Das, R., Granat, L., Leck, C., Praveen, P.S., 2011. Chemical composition of rainwater at
584 Maldives Climate Observatory at Hanimaadhoo (MCOH). Atmospheric Chemistry and
585 Physics, 11, 3743-3755.

586 deMenocal, P., 2005. Plio-Pleistocene African climate. Science, 270, 53-59.

587 deMenocal, P., 2004. African climate change and faunal evolution during the Pliocene-
588 Pleistocene. Earth and Planetary Science Letters, 220, 3-24.

589 van der Does, M., Knippertz, P., Zschenderlein, P., Giles Harrison, R., Stuut, J.-B., 2018. The
590 myterious long-range transport of giant mineral dust particles. Science Advances, 4,
591 eaau2768.

592 Droxler, A.W., Haddad, G.A., Mucciarone, D.A., and Cullen, J.L., 1990. Pliocene-Pleistocene
593 aragonite cyclic variations in Holes 714A and 716B (The Maldives) compared with Hole
594 633A (The Bahamas): records of climate-induced $CaCO_3$ preservation at intermediate water
595 depths. In: Duncan, R.A., Backman, J., Peterson, L.C., et al. (Eds), Proceedings of the Ocean
596 Drilling Program, Scientific Results, 115, 539-577.

597 Eck, T.F., Holben, B.N., Dubovik, O., Smirnov, A., Slutsker, I., Lobert, J.M., Ramanathan,
598 V., 2001. Column-integrated aerosol optical properties over the Maldives during the northeast
599 monsoon for 1998-2000. Journal of Geophysical Research, 106, 28555-28566.

600 Folk, R.L. and Ward, W.C., 1957. Brazos River bar; a study in the significance of grain size
601 parameters. Journal of Sedimentary Research, 27, 3-26.

602 Glaser, K. S., and Droxler, A. W., 1993, Controls and development of Late Quartenary
603 periplatform carbonate stratigraphy in Walton Basin (Northeastern Nicaragua Rise,
604 Carribbean Sea). Paleoceanography, 8, 243-274.

605 Glennie, K.W., Singhvi, A.K., Lancaster, N., Teller, J.T., 2002. Quaternary climatic changes
606 over Southern Arabia and the Thar Desert, India. In: Clift, P.D., Kroon, D., Gaedicke, C.,
607 Craig, J. (Eds), The Tectonic and Climatic Evolution of the Arabian Sea Region. Geological
608 Society, London, Special Publications, 195, 301-316.

609 Goddard, L. and Graham, N.E., 1999. Importance of the Indian Ocean for simulating rainfall
610 anomalies over eastern and southern Africa. Journal of Geophysical Research, 104, 19099-
611 19116.

612 Goswami, V., Singh, S.K., Bhushan, R., Rai, V.K., 2012. Temporal variations in $^{87}Sr/^{86}Sr$ and
613 □Nd in sediments of the southeastern Arabian Sea: Impact of monsoon and surface water
614 circulation. Geochemistry, Geophysics, Geosystems, 13, Q01001.

615 Gupta, A.K., Anderson, D.M., Overpeck, J.T., 2003. Abrupt changes in the Asian southwest
616 monsoon during the Holocene and their links to the North Atlantic Ocean. Nature 421, 354-
617 357.

618 Gupta, A.K., Yuvaraja, A., Prakasam, M., Clemens, S.C., Velu, A., 2015. Evolution of the
619 South Asian monsoon wind system since the late Middle Miocene. Palaeogeography,
620 Palaeoclimatology, Palaeoecology 438, 160-167.

621 Hammer, Ø., Harper, D.A.T., Ryan, P.D., 2001. PAST: paleontological statistics software
622 package for education and data analysis. Palaeontologia Electronica, 4, 9 pp.

623 Haug, G.H., Sigman, D.M., Tiedemann, R., Pedersen, T.F., Sarnthein, M., 1999. Onset of
624 permanent stratification in the subarctic Pacific Ocean. Nature, 401, 779-782.

625 Haywood, A.M., Dowsett, H.J., Dolan, A.M., 2016. Integrating geological archives and
626 climate models for the mid-Pliocene warm period. Nature Communication, 7, 10646.

627 Huybers, P. and Eisenman, I., 2006. Integrated summer insolation calculations. IGBP
628 PAGES/World Data Center for Paleoclimatology Data Contribution Series # 2006-079.
629 NOAA/NCDC Paleoclimatology Program, Boulder CO, USA.

630 Innocent, C., Fagel, N., Hillaire-Marcel, C., 2000. Sm-Nd isotope systematics in deep-sea
631 sediments: clay-size versus coarser fractions. Marine Geology 168, 79-87.

632 Jung, S.J.A., Davies, G.R., Ganssen, G.M., Kroon, D., 2004. Stepwise Holocene aridification
633 in NE Africa deduced from dust-borne radiogenic isotope records. Earth and Planetary
634 Science Letters, 221, 27-37.

635 Kessarkar, P.M., Rao, V.P., Ahmad, S.M., Babu, G.A., 2003. Clay minerals and Sr-Nd
636 isotopes of the sediments along the western margin of India and their implication for sediment
637 provenance. Marine Geology 202, 55-69.

638 Kolla, V., Kostecki, J., Robinson, F., Biscaye, P., Ray, P., 1981. Distribution and origins of
639 clay minerals and quartz in surface sediments of the Arabian Sea. Journal of Sedimentary
640 Research, 51, 563-569.

641 Kroon, D., Steens, T., Troelstra, S.R., 1991. Onset of monsoonal related upwelling in the
642 western Arabian Sea as revealed by planktonic foraminifers. In: Prell, W.L., Niitsuma, N., et
643 al., (Eds), Proceedings of the Ocean Drilling Program, Scientific Results, 117, 257-263.

644 Kunkelova, T.; Jung, S., de Leau, E., Odling, N., Thomas, A., Betzler, C., Eberli, G., Alvarez-
645 Zarikian, C., Alonso-García, M., Bialik, O., Blättler, C., Guo, J., Haffen, S., Horozal, S., Ling
646 Hui Mee, A.; Inoue, M., Jovane, L., Lanci, L., Laya, J., Lüdmann, T., Nath, N., Nakakuni, M.,
647 Niino, K., Petruny, L., Pratiwi, S., Rijmer, J., Reolid, J., Slagle, A., Sloss, C., Su, X., Swart,
648 P., Wright, J., Yao, Z., Young, J., Lindhorst, S., Hayman-Stainbank, S., Rüggeberg, A.,
649 Spezzaferri, S., Carrasqueira, I., Yu, S., Kroon, D., 2018. A two million year record of low
650 latitude aridity linked to continental weathering from the Maldives. Progress in Earth and
651 Planetary Science, 5, 86.

652 Kurian, J. and Vinayachandran, P.N., 2007. Mechanisms of formation of the Arabian Sea
653 mini warm pool in a high-resolution Ocean General Circulation Model. Journal of
654 Geophysical Research, 112: C05009.

655 Lanci, L., Zanella, E., Jovane, L., Alonso-García, M., Alvarez-Zarikian, C.A., Betzler, C.,
656 Bialik, O.M., Blättler, C.L., Eberli, G.P., Guo, J.A., Haffen, S., Horozal, S., Inoue, M., Kroon,
657 D., Laya, J.C., Ling Hui Mee, A., Lüdmann, T., Nakakuni, M., Bejugam, N.N., Niino, K.,
658 Petruny, L.M., Pratiwi, S.D., Reijmer, J.J.G., Reolid, J., Slagle, A.L., Sloss, C.R., Su, X.,
659 Swart, P.K., Wright, J.D., Yao, Z., Young, J.R., submitted. Magnetic properties of Early
660 Pliocene sediments from IODP Site 2U1467 (Maldives platform) reveal changes in the
661 monsoon system. Palaeogeography, Palaeoclimatology, Palaeoecology.

662 Laskar, J., P. Robutel, F. Joutel, M. Gastineau, A.C.M. Correia, B. Levrard, 2004. A long-
663 term numerical solution for the insolation quantities of the Earth. Astronomy and
664 Astrophysics 428, 261-285.

665 Léon, J.-F. and Legrand, M., 2003. Mineral dust sources in the surrounding of the north
666 Indian Ocean. Geophysical Research Letters, 30, 1309.

667 Lisiecki, L. E. and Raymo, M.E., 2005, A Pliocene-Pleistocene stack of 57 globally
668 distributed benthic d18O records, Paleoceanography, 20, PA1003.

669 Lindhorst, S., Betzler, C., Wunsch, M., Lüdmann, T., Kuhn, G., 2019. Carbonate drifts as
670 marine archives of aeolian dust (Santaren Channel, Bahamas). Sedimentology, doi:
671 10.1111/sed.12576

672 Lüdmann, T., Kalvelage, C., Betzler, C., Fürstenau, J., Hübscher, C., 2013. The Maldives, a
673 giant isolated carbonate platform dominated by bottom currents. Marine and Petroleum
674 Geology, 43, 326-340.

675 McCave, I.N., Manighetti, B. and Robinson, S.G. 1995. Sortable silt and fine sediment
676 size/composition slicing: parameters for palaeocurrent speed and palaeoceanography.
677 Paleoceanography, 10, 593-610.

678 Meyer, I., Davies, G.R., Stuut, J.B.W., 2011. Grain size control on Sr-Nd isotope provenance
679 studies and impact on paleoclimate reconstructions: An example from deep-sea sediments
680 offshore NW Africa. Geochemistry, Geophysics, Geosystems, 12, 1-14.

681 Middleton, N.J., 1986a. A geography of dust storms in south-west Asia. Journal of
682 Climatology, 6, 183-196.

683 Middleton, N.J., 1986b. Dust storms in the Middle East. Journal of Arid Environments, 10,
684 83-96.

685 Miller, K.G., Kominz, M.A., Browning, J.V., Wright, J.D., Mountain, G.S., Katz, M.E.,
686 Sugarman, P.J., Cramer, B.S., Christie-Blick, N., Pekar, S.F., 2005. The Phanerozoic record
687 of global sea-Level change. Science, 310, 1293-1298.

688 Nair, R.R., Ittekkot, V., Manganini, S.J., Ramaswamy, V., Haake, B., Degens, E.T., Desai,
689 B.N., Honjo, S., 1989. Increased particle flux to the deep ocean related to monsoons. Nature,
690 338, 749-751.

691 Nie, J., 2017. The Plio-Pleistocene 405-kyr climate cycles. Palaeogeography,
692 Palaeoclimatology, Palaeoecology, 510, 26-30.

693 Paillard, D., Labeyrie, L., Yiou, P., 1996. Macintosh Program performs time-series analysis.
694 Eos, 77, 379.

695 Paul, A., Reijmer, J. J. G., Fürstenau, J., Kinkel, H., and Betzler, C., 2012, Relationship
696 between Late Pleistocene sea-level variations, carbonate platform morphology and aragonite
697 production (Maldives, Indian Ocean). Sedimentology, 59, 1540-1658.

698 Prell, W.L. and van Campo, E., 1986. Coherent response of Arabian Sea upwelling and pollen
699 transport to Late Quaternary monsoonal winds. Nature, 323, 526-528.

Prospero, J.M., Bonatti, E., Schubert, C., Carlson, T.N., 1970. Dust in the Caribbean atmosphere traced to an African dust storm. Earth and Planetary Science Letters, 9, 287-293.

Prospero, J.M., Ginoux, P., Torres, O., Nicholson, S.E., Gill, T.E., 2002. Environmental characterization of global sources of atmospheric soil dust identified with the Nimbus 7 Total Ozone Mapping Spectrometer (TOMS) Absorbing Aerosol product. Reviews of Geophysics, 40, 1002.

Purdy, E.G. and Bertram, G.T., 1993. Carbonate Concepts from the Maldives, Indian Ocean. AAPG Studies in Geology, 34.

Ramaswamy, V., 2014. Influence of tropical storms in the northern Indian Ocean on dust entrainment and long-range transport. In: Tang and Sui (Eds), Typhoon impact and crisis management. Advances in Natural and Technological Hazard Research, 40, 149-174.

Ramaswamy, V., Muraleedharan, P.M., Babu, P., 2017. Mid-troposphere transport of Middle-East dust over the Arabian Sea and its effect on rainwater composition and sensitive ecosystems over India. Scientific Reports, 7, 13676.

Rodgers, K.B., Latif, M., Legutke, S., 2000. Sensitivity of equatorial Pacific and Indian Ocean watermasses to the position of the Indonesian throughflow. Geophysical Research Letters, 27, 2941-2945.

Shackleton, N.J., Backman, J., Zimmerman, H., Kent, D.V., Hall, M.A., Roberts, D.G., Schnitker, D., Baldauf, J.G., Desprairies, A., Homrighausen, R., Huddlestun, P., Keene, J.B., Kaltenback, A.J., Krumsiek, K.A.O., Morton, A.C., Murray, J.W., Westberg-Smith, J., 1984. Oxygen isotope calibration of the onset of ice-rafting and history of glaciation in the North Atlantic region. Nature, 307, 620-623.

Shankar, D., Vinayachandran, P.N., Unnikrishnan, A.S., 2002. The monsoon currents in the north Indian Ocean. Progress in Oceanography 52, 63-120.

Sharifi, A., Murphy, L.N., Pourmand, A., Clement, A.C., Canuel, E.A., Beni, A.N., Lahijani, H.A., Delanghe, D., Ahmady-Birgani, H., 2018. Early-Holocene greening of the Afro-Asian dust belt changed sources of mineral dust in West Asia. Earth and Planetary Science Letters, 481, 30-40.

Shetye, S.R., 1998. West India Coastal Current and Lakshadweep High/Low. Sadhana, 23, 637-651.

730 Sirocko, F. and Sarnthein, M., 1989. Wind-borne deposits in the northwestern Indian Ocean:
731 record of Holocene sediments versus modern satellite data. In: Leinen, M. and Sarnthein, M.
732 (Eds), Paleoclimatology and Paleometeorology: Modern and Paste Pattern of Global
733 Atmospheric Transport. Kluwer Academic, Dordrecht, The Netherlands, 401-433.

734 Skonieczny, C., McGee, D., Winckler, G., Bory, A., Bradtmiller, L.I., Kinsley, C.W.,
735 Polissar, P.J., De Pol-Holz, R., Rossignol, L., Malaizé, B., 2019. Monsoon-driven Saharan
736 dust variability over the past 240,000 years. Science Advances, 5, eaav1887.

737 Stone, E.A., Lough, G.C., Schauer, J.J., Praveen, P.S., Corrigan, C.E., Ramanathan, V., 2007.
738 Understanding the origin of black carbon in the atmospheric brown cloud over the Indian
739 Ocean. Journal of Geophysical Research, 112, D22S23.

740 Sun, Y.B., An, Z.S., Clemens, S.C., Bloemendal, J., Vandenberghe, J., 2010. Seven million
741 years of wind and precipitation variability on the Chinese Loess Plateau. Earth and Planetary
742 Science Letters, 297, 525-535.

743 Tanaka TY and Chiba M, 2006. A numerical study of the contributions of dust source regions
744 to the global dust budget. Global and Planetary Change, 52, 88-104.

745 Tomczak, M. and Godfrey, J.S., 2003. Regional Oceanography: An Introduction. Daya
746 Publishing House, Delhi.

747 Tsoar, H. and Pye, K., 1987. Dust transport and the question of desert loess formation.
748 Sedimentology, 34, 139-153.

749 Wyrtki, K. (1973). Physical oceanography of the Indian Ocean. In: Zeitschel (Ed), The
750 biology of the Indian Ocean. Springer-Verlag, New York.

751 Yu, Y., Notaro, M., Kalashnikova, O.V., Garay, M.J., 2015. Climatology of summer Shamal
752 wind in the Middle East. Journal of Geophysical Research: Atmosphere, 121, 289-305.

753 Zhang, Y.G., Ji, J., Balsam, W., Liu, L., Chen, J., 2009. Mid-Pliocene Asian monsoon
754 intensification and the onset of Northern Hemisphere glaciation. Geology, 37, 599-602.

755

756 Figure Captions

757

758 **Fig. 1: A, B)** Location of the study site in the Indian Ocean; WICC: West India Coastal
759 Current during northern hemisphere winter months (after Shetye, 1998); **C)** Multibeam

760 bathymetry of the Maldives' Inner Sea surrounding the IODP expedition 359 drilling site
761 U1467. Red dot marks position of IODP site U1467.

762

763 **Fig. 2: A)** Age-depth plot for site U1467 splice section. Depths are given in metres of core
764 depth (mcd) with reference to the CCSF-359-U1467-ABCD-20160114 depth scale. Green
765 dots and named biostratigraphic events refer to the biostratigraphy as reported by Betzler et al.
766 (2017). Please note that depths of biostratigraphic tie points are midpoints depths, recalculated
767 to mcd. Grey dots are age tie points derived from correlating bulk grain-size data of U1467
768 (this work) against long-term sea-level data (Miller et al., 2005). See methods section for
769 details.

770

771 **Fig. 3: A)** Summer insolation for 65°N and sea-level data of Miller et al. (2005); **B)** Results
772 of grain-size analyses of the bulk and the terrigenous sediment fraction of site U1467
773 sediments: Percentage of bulk mud ($Bulk_{\%mud}$); percentage of terrigenous particles in the size
774 range 8-63 µm ($TF_{\%8-63}$); size of largest terrigenous particles (TF_{d90}); mean grain size of the
775 terrigenous fraction <63 µm ($TF_{Mean\ <63}$). Main global climate events are indicated for
776 orientation: Middle Pleistocene Transition (MPT; 1.25-0.75 Ma; Clark et al., 2006); mid
777 Pliocene warm period (mPWP; 3.3-3.0 Ma; Haywood et al., 2016); onset of extensive
778 northern Hemisphere glaciation (since 2.7 Ma; Shackleton et al., 1984; Haug et al., 1999);
779 closure of Indonesian seaway (4.0-3.0 Ma; Cane and Molnar, 2001).

780

781 **Fig. 4:** Wavelet spectra for the terrigenous fraction of site U1476 samples for **A)** percentage
782 of terrigenous particles falling into the 8-63 µm size range ($TF_{\%8-63}$); and **B)** size of the
783 coarsest particles (TF_{d90}).

Highlights of “Wind variability over the northern Indian Ocean during the past 4 million years – insights from coarse aeolian dust (IODP Exp. 359, Site U1467, Maldives)”:

- A 4 Myr record of coarse aeolian dust transport over the Indian Ocean is presented
- Shamal winds are responsible for long-range coarse dust transport
- Data show particle-size dependence of provenance of terrigenous material
- Variability of dust transport shows eccentricity control (400 kyr and 100 kyr)
- Transport of coarse dust is rather prone to wind speed than to source area aridity

Wind variability over the northern Indian Ocean during the past 4 million years – insights from coarse aeolian dust (IODP Exp. 359, Site U1467, Maldives)

Sebastian Lindhorst[1], Christian Betzler[1], Dick Kroon[2]

[1] Universität Hamburg, Zentrum für Erdsystemforschung und Nachhaltigkeit CEN, Institut für Geologie, Bundesstr. 55, 20146 Hamburg, Germany; sebastian.lindhorst@uni-hamburg.de

[2] School of GeoSciences, Grant Institute, University of Edinburgh, The King's Buildings, West Mains Road, Edinburgh EH9 3JW, United Kingdom

Abstract

The lithogenic fraction of carbonate drift sediments from IODP Exp. 359 Site U1467 (Maldives) provides a unique record of atmospheric dust transport over the northern Indian Ocean during the past 4 Myr. Grain-size data provide proxies for dust flux (controlled by source area aridity) as well as wind transport capacity (wind speed). Entrainment and long-range transport of dust in the medium to coarse silt size range is linked to the strength of the Arabian Shamal winds and the occurrence of convective storms which prolong dust transport. Dust flux and the size of dust particles increased between 4.0 and 3.3 Ma, corresponding to the closure of the Indonesian seaway and the intensification of the South Asian Monsoon. There is no clear trend in dust flux between 3.3 and 1.6 Ma, whereas wind transport capacity decreased. Between 1.6 Ma and the Recent, dust flux increased and shows higher variability, especially during the last 500 kyr. Transport capacity increased between 1.2 and 0.5 Ma and slightly decreased since then. Frequency analysis shows that dust transport varies on orbital timescales, with eccentricity control being the most prominent (400 kyr throughout the record, 100 kyr between 2.0 and 1.3 Ma, and since 1.0 Ma). Higher frequency cycles (obliquity and precession) are more pronounced in wind transport capacity than in the amount of dust. This indicates that the amount of coarse dust in sediments from the Maldives as a far-field site is more prone to changes in transport mechanisms than to changes in dust source-area aridity.

Keywords: climate archive, dust, grain size, carbonate drift, South Asian Monsoon, Shamal wind

1. Introduction

Knowledge of the past wind regime over the northern Indian Ocean, so far, comes from the source-proximal Arabian Sea dust records, the isotopic composition of planktonic foraminifera, or is based on data from upwelling areas, where increased productivity is linked to intensified surface winds (Sirocko and Sarnthein, 1989; Kroon et al., 1991; Clemens, 1998; Gupta et al., 2003; 2015). Records of the long-term evolution of the wind field over the northern Indian Ocean are scarce. This study aims to fill this gap by investigating the terrigenous residue of carbonate-drift sediments, which provide an excellent archive of aeolian dust, including the coarse dust fraction, and are unaffected by size sorting effects of oceanic bottom currents (Lindhorst et al., 2019).

Main sources of mineral dust supplied to the western Arabian Sea are the Nubian Desert, the Arabian Peninsula, and desert areas in Iran, Pakistan and Afghanistan as well as in North West India (Middleton, 1986a; Clemens, 1998; Prospero et al., 2002; Léon and Legrand, 2003; Fig. 1). There is an inter-annual latitudinal shift of dust entrainment with low latitudinal sources being active in the winter and higher latitudinal sources becoming more active in late spring and summer (Prospero et al., 2002). Entrainment of dust in Africa and areas located in the inner Arabian Peninsula is largest in spring and summer, whereas in autumn, dust emission is more restricted to the coastal parts of Oman and Somalia (Glennie et al., 2002; Léon and Legrand, 2003). Dust export from the Thar Desert and other areas along the border of Pakistan and India is greatest in summer and autumn (Middleton, 1986a).

Main drivers for dust entrainment in the Arabian Peninsula are the southwest-winds of the summer monsoon and dust-loaded Shamal winds from north-westerly direction (Glennie et al., 2002; Fig. 1). Shamal winds develop along the pressure gradient between the low-pressure monsoon system over India and the high-pressure system over the eastern Mediterranean and are further enhanced by orographic effects along the Persian Gulf (Middleton, 1986b). These winds can override the moist near-surface winds of the southwest monsoon and transport large quantities of dust towards the eastern Arabian Sea, where it is scavenged by summer monsoonal precipitation and wet-deposited (Ackerman and Cox, 1989; Sirocko and Sarnthein,

1989; Yu et al., 2015; Ramaswamy et al., 2017). This process of mid-tropospheric transport also results in a prolonged transport of dust towards the Bay of Bengal and the equatorial Indian Ocean (Ramaswamy et al., 2017; Clemens, 1998). Shamal winds occur in summer as well is in winter, but dust activity is mainly related to the summer Shamal (Yu et al., 2015). Dust transport over the northern Indian Ocean is also prone to the occurrence of tropical cyclones, which can alter the trajectories of dust particles, but can also foster dust entrainment during seasons otherwise characterized by low wind speeds (Ramaswamy, 2014).

In the western Arabian Sea the flux of lithogenic particles is 1.5 to 6 times higher during the southwest (summer-) monsoon (June to September) than during the northeast (winter-) monsoon (December to February), with this gradient being more pronounced in the eastern Arabian Sea (Nair et al., 1989). However, these data did not allow distinguishing aeolian and riverine input and may contain a significant portion of suspended matter supplied by the large rivers draining into the eastern Arabian Sea as this is indicted by radiogenic isotope composition of the sediment that show that the majority of Indus River sediment is deposited in the northern Arabian Sea (Kessarkar et al., 2003).

In this study, a four million year record of aeolian dust transport over the northern Indian Ocean obtained from the terrigenous fraction of carbonate-dominated drift sediments of the Maldives archipelago is presented. Carbonate drifts were deposited in the Maldives Inner Sea, a perched basin, largely isolated from riverine input of coarse material (Kolla et al., 1981; Bunzel et al., 2017; Betzler et al., 2018; Kunkelova et al., 2018).

2. Study site

The Maldives archipelago is an isolated tropical carbonate platform located southwest of India in the northeastern Indian Ocean (Fig. 1). The Maldives carbonate succession accumulated since the Eocene (Aubert and Droxler, 1992; Purdy and Bertram, 1993). Nowadays, the platform is composed of a double row of atolls that enclose a sedimentary basin, the Maldives Inner Sea, which has served as a natural sediment trap of current controlled deposits since the Middle Miocene (Betzler et al., 2017, 2018). Water depths in the Inner Sea are between 300 and 600 m and marine passages, up to several hundreds of metres deep, connect the Inner Sea with the open Indian Ocean, where water depths reach more than 2000 m in the immediate vicinity of the carbonate platform. Due to the bathymetric gradient,

96 the Maldives Inner Sea represents an isolated perched basin, elevated with regard to the
97 surrounding ocean floor. In consequence, terrigenous input in the Maldives sedimentary
98 record is largely restricted to aeolian transported dust, with a minor component of fluvial
99 derived material delivered by currents from the Arabian Sea and the Bay of Bengal (Kolla et
100 al., 1981). Sedimentation in the Inner Sea is locally controlled by contour currents that
101 accumulate large carbonate drift bodies composed of periplatform ooze around atolls and
102 drowned banks (Betzler et al., 2009, 2013a, 2013b; Lüdmann et al., 2013).

103 Since around 12.9 Ma, climate and oceanographic setting of the Maldives are controlled
104 by the bi-directional, seasonally reversing South Asian Monsoon system (Wyrtki, 1973;
105 Tomczak and Godfrey, 2003; Betzler et al., 2016). Winds from the southwest prevail during
106 the Northern Hemisphere summer (April to November), whereas northeasterly winds
107 predominate during the winter (November to April). Atmospheric circulation over the
108 Arabian Sea is stronger during the summer monsoon than during the winter monsoon; roughly
109 by a factor of three (Clemens, 1998). Annual precipitation is around 900 mm yr^{-1}; with
110 highest amounts in the summer months (July to September).

111 The direction of surface ocean currents in the northern Indian Ocean seasonally reverses
112 with the wind system, and are westward-directed in winter and eastward in summer (Shankar
113 et al., 2002). Part of this current system are surface currents that flow along the Indian coast:
114 from the Bay of Bengal to the south-eastern Arabian Sea during winter (West India Coastal
115 Current, WICC; Fig. 1) and vice versa during summer (Shetye, 1998; Shankar et al., 2002;
116 Kurian and Vinayachandran, 2007).

117 The Maldives are located close to the world's largest sources of dust: North Africa and the
118 Arabian Peninsula providing 58 and 12 wt% of the global dust emissions, respectively
119 (Tanaka and Chiba, 2006). The main input of aeolian dust into the Arabian Sea and towards
120 the northern Indian Ocean is linked to the prevailing southwest winds during the summer
121 monsoon and subordinated north-westerly Shamal winds (Clemens, 1998; Ackerman and
122 Cox, 1989; Nair et al., 1989; Prospero et al., 2002; Yu et al., 2015; Ramaswamy et al., 2017;
123 Banerjee et al., 2019). These winds entrain dust from the arid areas in northeast Africa and the
124 Arabian Peninsula, which is subsequently scavenged by monsoonal rains into the ocean. By
125 contrast, satellite based measurements on the aerosol optical thickness show that the modern
126 dust plume of the winter monsoon clearly reaches the Maldives (Kunkelova et al., 2018).
127 Measurements at the Maldives Climate Observatory at Hanimaadhoo Atoll in the northern
128 Maldives and numerical models of the seasonality of aerosol loadings in south Asia underline

this seasonality in the composition and provenance of aerosols: highest concentrations of (coarse) mineral dust from April to September, whereas fine dust including sulphate and black carbon of anthropogenic origin reach peak concentrations from November to January with the portion of coarse minerogenic dust being by far lower than during the rest of the year (Eck et al., 2001; Chowdhury et al., 2001; Stone et al., 2007; Adhikary et al., 2007; Das et al., 2011).

IODP (Integrated Ocean Drilling Program) site U1467 (4°51.0274′N, 73°17.0223′E, water depth 487.4 m) was drilled during Expedition 359 in October 2015. Site U1467 recovered a 630 m thick sequence of pelagic carbonate drift deposits from the eastern Inner Sea of the Maldives and provides a well-preserved, continuous record of lithogenic input into the south-eastern Arabian Sea (Betzler et al., 2017; Kunkoleva et al., 2018).

3. Methods

Sampling of IODP Exp. 359 Site U1467 cores was done in April and May 2016 under the sample request 29856IODP. Sampling followed the shipboard splice information (splice-359-U1467-BCD-20160114; IODP LIMS Database: http://iodp.tamu.edu/database/) and comprised samples of 10 cm^3 each. All depth readings in this work refer to the depth scale CCSF-359-U1467-ABCD-20160114) and are given in metres of composite depth (mcd).

3.1 Grain-size analysis and statistics

Samples for bulk grain size were wet sieved (2000 μm) prior to measurement to remove very coarse particles like coral detritus and large pteropod shells. Samples for the determination of the terrigenous grain-size spectrum were wet sieved using a 63 μm sieve to remove the larger carbonate particles. Chemical treatment followed the workflow described by McCave et al. (1995): the bulk fraction < 63 μm was heated in H_2O_2 to oxidize the organic portion, and subsequently treated with 1M Ca_3COOH (acetic acid) to dissolve the carbonate. Biogenic opal was removed with 2M $NaHCO_3$ (sodium bicarbonate). Samples of the terrigenous residue were visually inspected by means of a binocular microscope to ensure complete dissolution of carbonate and biogenic silica as well as complete disintegration of aggregates. Prior to grain-size measurement, all samples were dispersed in water using

ultrasonic and 0.05% $Na_4P_2O_7$ x 10 H_2O (tetra-sodium diphosphate decahydrate) as dispersing agent. Measurements were done using a Sympatec Helos KFMagic laser particle-size analyser and measuring ranges of 0.5/18-3500 µm for bulk grain size and 0.25-87.5 µm for the non-carbonate residual, respectively. To ensure accuracy of measurements and absence of a long-term instrumental drift, an in-house grain-size standard was measured daily prior to the series of measurements (standard deviation was <0.1 µm for the measuring range 0.25-87.5 µm and <3.3 µm for 0.5/18-3500 µm, respectively).

Grain-size statistics are based on the graphical method (Folk and Ward, 1957) and were calculated using Gradistat (Blott and Pye, 2001). Values for percentages are rounded to the nearest integer. Correlation coefficients are based on the Spearman rank correlation, as this method supports nonlinear correlations.

Below 174.34 mcd (metres core depth) deposits at IODP Exp. Site U1467 show chert concretions. These aggregates could not be disintegrated by means of chemical treatment and as a consequence caused an apparent coarsening of the grain-size spectrum. All grain-size data from below 174.10 mcd (corresponding to a depositional age of 4.0 Ma) are therefore excluded from further interpretation.

3.2 Age model

The initial age framework for Site U1467 samples is based on biostratigraphic (calcareous nannofossils and planktonic foraminifera) and magnetostratigraphic data as provided by Betzler et al. (2017). The early Pliocene part of the biostratigraphic age model (from 3.1 Ma) is in good agreement with magnetic stratigraphic data from the same site (Lanci et al., this volume). The long-term averaged sedimentation rate is 3.4 cm kyr^{-1} for the last 4 Myr (Betzler et al., 2017). This does not take into account that periplatform carbonates show variable sedimentation rates reflecting the flooding or emersion of the banks and atolls surrounding the Inner Sea and consequently the export of shallow-water material from these areas. This effect is especially pronounced with the inception of the high amplitude sea-level variations for the past 0.75 Myr after the Mid-Pleistocene Transition (MPT). To overcome this shortcoming, we correlate the bulk grain-size data of Site U1467 with the sea-level data of Miller et al. (2005) and the global oxygen isotope stack LR04 (Lisiecki and Raymo, 2004): finer grained periplatform ooze forms during sea-level highstand when the platforms export large amount of carbonate (Boardmann et al., 1986, Glaser and Droxler, 1993). For the Maldives, the validity of this assumption has been shown by Paul et al. (2012) and Bunzel et al. (2017).

193 Correlation was done by manual correlation of minima in bulk grain size and sea-level lows.
194 Subsequently, local highs in sea level were linked with corresponding fine peaks in bulk grain
195 size.

196 Correlations and all time-depth conversions were done using Analyseries 2.0.8 (Paillard et
197 al., 1996). Wavelet spectra were calculated with PAST (Hammer et al., 2001), same for
198 insolation data, where the algorithms of Laskar et al. (2004) and the data of Huybers and
199 Eisenman, (2006) have been used. Sample size for wavelet spectra is 0.007 Myr.

200

201 # 4. Results

202

203 ## 4.1 Age model

204 The final age model for Site U1467 samples accounts for the carbonate-productivity
205 controlled variability of the sedimentation rate on orbital time scales. Sedimentation rates for
206 Site U1467 are 1.0 to 26.5 cm kyr^{-1}, with a median of 3.8 cm kyr^{-1} (Fig. 2). In general,
207 sedimentation rates are higher and less variable in the older part of the record, compared to
208 the youngest part: sedimentation rates of 1.6 to 9.3 cm kyr^{-1} (median 5.9 cm kyr^{-1}) between
209 4.0 to 3.0 Ma contrast with rates of 1.0 to 26.5 cm kyr^{-1} (median 4.7 cm kyr^{-1}) between 1.0 Ma
210 and the Recent.

211

212 ## 4.2 Grain-size distribution

213 Sample recovery and using our age model resulted in time-variable sample intervals of
214 0.0009-0.039 Myr (median 0.0053 Myr) and 0.0009-0.0778 Myr (median 0.0055 Myr) for
215 bulk grain size and terrigenous residue, respectively. Each sample (thickness c. 1.5 cm)
216 represents the integrated sedimentation over a period of 290 yrs (range 57 to 1,500 yrs), on
217 average.

218 The portion of mud-size particles (< 63 µm; $Bulk_{\%Mud}$) varies between 28 and 100 % of
219 the bulk fraction with a median of 77 % (Fig. 3). The highest mud contents (> 95 %) are in the
220 oldest part of the record (4.0-3.6 Ma) and around 2.0 Ma; lowest mud contents occur between
221 2.4-2.1 and around 1.0 Ma. There is an overall coarsening of the bulk fraction starting at 4.0
222 Ma until reaching the absolute minimum in $Bulk_{\%Mud}$ around 2.3 Ma, which is followed by a
223 rapid fining until 2.0 Ma. $Bulk_{\%Mud}$ stays around 80 % until 1.05 Ma, where an abrupt

224 coarsening starts. Subsequently, and until the Recent, there is an overall fining, superimposed
225 by pronounced higher frequency changes with amplitudes of 20 % and greater.

226 The grain size of the terrigenous fraction is characterized by the 90th percentile of the
227 grain-size spectrum < 63 µm (TF_{d90}) and the percentage of particles in the grain-size range 8
228 to 63 µm ($TF_{\%8-63}$). TF_{d90} serves as a measure for the coarsest particles in this size range and,
229 with respect to dust, provides information on wind transport capacity (i.e. wind speed). In
230 addition, $TF_{\%8-63}$ is regarded as a proxy for the total amount of dust in the medium to coarse
231 silt range (here referred to as coarse dust). The mean grain size of the terrigenous fraction <63
232 µm is provided for comparison (Fig. 3).

233 At Site U1467, $TF_{\%8-63}$ ranges from 28 to 68 %, with a median of 48 %. Lowest
234 percentages are present prior to 3.6 Ma and highest values occur around 3.3 Ma and in the
235 youngest part of the record, i.e. the past 0.6 Myr. There is an overall coarsening of the
236 terrigenous fraction throughout the record, and with respect to long-term trends, different
237 periods can be distinguished: A coarsening from 4.0 to 3.3 Ma is followed by a rapid decrease
238 of the amount of coarse dust until 3.1 Ma. Between 3.1 and 2.4 Ma, there is no clear trend.
239 Subsequently, until 1.8 Ma, $TF_{\%8-63}$ increases, before it reaches a minimum around 1.6 Ma.
240 Afterwards, there is a coarsening until 0.6 Ma. The youngest period, 0.6 Ma to the Recent is
241 characterized by a high variability of the amount of coarse particles.

242 The mean grain size of the terrigenous fraction <63 µm ($TF_{Mean\ <63}$) varies between 2.7
243 and 8 µm (median 3.8 µm); the size of the coarsest particles in the terrigenous fraction (TF_{d90})
244 ranges from 9.4 to 21.4 µm (median 13.4 µm). TF_{d90} is finest prior to 3.8 Ma and coarsest
245 around 3.3 Ma. With regard to long-term trends, three intervals can be distinguished: first, a
246 coarsening until 3.3 Ma, followed by, second, an overall fining until 1.6 Ma, and subsequently
247 a coarsening of TF_{d90} until today.

248 Visually, the curves of $TF_{\%8-63}$ and TF_{d90} appear to have a similar shape. The
249 mathematical correlation of both curves, however, is only 0.6 ($p < 0.0001$) and long-term
250 trends are slightly different. $TF_{\%8-63}$ and TF_{d90} both show a coarsening from 4.0 to 3.3 Ma.
251 Subsequently, the size of the coarsest particles slightly decreases until 1.2 Ma, whereas their
252 percentage remains stable until 1.6 Ma. The overall coarsening in the younger part of the
253 record starts around 1.6 Ma if $TF_{\%8-63}$ is considered, and later, at 1.2 Ma, if the absolute size
254 of the largest particles (TF_{d90}) is taken as a measure.

255 The wavelet spectra of both, $TF_{\%8-63}$ and TF_{d90}, show the presence of cyclic variability on
256 orbital timescales (Fig. 4). Frequencies in the precessional (23 kyr) and the obliquity (41 kyr)

band are more pronounced in the size of the coarsest particles (TF_{d90}), than in the percentage of coarse particles ($TF_{\%8-63}$). The short eccentricity cycle (100 kyr) is present in both grain-size parameters after 2.0 Ma, but weakens between 1.6 and 1.0 Ma ($TF_{\%8-63}$) and 1.3 and 1.0 Ma (TF_{d90}), respectively. The influence of the short eccentricity cycle is also weak in the older part of the record. The long eccentricity cycle with a frequency of around 400 kyr is present in both datasets, but weak prior to 2.0 Ma in the $TF_{\%8-63}$ record, whereas it persists throughout the record in the TF_{d90} data.

5. Discussion

5.1 Bulk sediment grain size

Site U1467 has been cored in carbonate drifts consisting of periplatform ooze formed through off-bank transport of carbonate particles from the shallow water carbonate factories and pelagic carbonate- and silica production. We interpret the bulk grain-size data to reflect varying input from these sources. In general, a fining of carbonate drift sediments is expected during sea-level highstands, when export of mud-size particles from shallow-water banks and atolls is at its maximum (Boardmann et al., 1986, Droxler et al., 1990; Glaser and Droxler, 1993; Paul et al., 2012). Coarsening, by contrast, occurs when sea level is low and banks and atolls emerge. In addition to this higher frequency variability interpreted to be triggered by sea-level, there are long-term trends in the bulk grain size from Site U1467 that do not correlate with published sea-level records (Fig. 3). The origin of these changes in bulk grain size has to remain speculative until a detailed analysis of the components is available. Such data would not only allow quantifying shallow-water and pelagic origin of carbonate particles, but also detecting changes in the water masses that bath the carbonate platform.

5.2 Glacial-interglacial variability and provenance of coarse dust

Studies on the dust records of the Arabian Sea and elsewhere have shown that lithogenic grain size is a reliable measure for wind transport capacity (i.e. wind speed), whereas the amount of dust, as indicated by lithogenic mass accumulation rates and the percentage of the lithogenic component, is controlled by source area aridity rather than transport energy (Prell and van Campo, 1986; Tsoar and Pye, 1987; Clemens and Prell, 1990; Clemens et al., 1991).

288 This study focuses on aeolian transported dust in the medium to coarse silt range (coarse
289 dust). The grain-size distribution of the terrigenous residue is characterized by i) the size of
290 the 90th percentile of the size range 8-63 µm (TF_{d90}) as a measure for the largest particles, and
291 ii) the percentage of particles in the size range 8-63 µm ($TF_{\%8-63}$) in relation to the total
292 amount of terrigenous particles < 63 µm. The clay and fine silt fraction (< 8 µm) has been
293 excluded to avoid bias due to the presence of the clay and fine dust particles which potentially
294 would mask subtle changes in the medium to coarse silt fraction (Lindhorst et al., 2019). This
295 dominance of the fine particles is illustrated by the comparable little variability in the mean
296 grain size of the particle spectrum < 63 µm (Fig. 3).

297 The variability of the lithogenic component of Maldivian carbonate drift sediments, as
298 recorded by element ratios derived by means of x-ray fluorescence (XRF) core scanning, has
299 been previously linked to precipitation changes in the dust source areas which are controlled
300 by the monsoonal system (Bunzel et al., 2017; Kunkelova et al., 2018). During glacial
301 periods, reduced precipitation and the intensification of the winter monsoon winds (from the
302 NE) causes increased mechanical weathering in the source areas and leads to higher dust flux
303 rates. Interglacial periods, by contrast, are characterized by more humid conditions due to a
304 stronger summer monsoon (winds from the SW), which results in higher continental discharge
305 rates, the intensification of chemical weathering, and increased input of fluvial material into
306 the ocean, whereas aeolian dust flux is expected to be reduced. Same is valid for the western
307 Arabian Sea, where dust flux as indicated by mass accumulation rates positively correlates
308 with global ice volume and as such is increased during glacial times (Clemens and Prell,
309 1990). Dust particle size, a measure for transport capacity, by contrast, varies on shorter time
310 scales and appears to be decoupled from dust flux (Clemens and Prell, 1990). Such a
311 decoupling of dust flux and transport capacity has also been observed in trans-Atlantic dust
312 transport, where it is interpreted to reflect the variability of different transport mechanisms
313 responsible for fine and coarse dust transport, respectively (Lindhorst et al., 2019).

314 Comparison of the Arabian Sea dust records and the XRF-based data from the Maldives,
315 with the grain-size data of the coarse dust fraction of Site U1467 presented in this study
316 reveals a different picture. During glacial periods, the total amount of dust, as traced by the
317 percentage of particles falling into the 8-63 µm size range, decreases and particles are finer
318 (smaller TF_{d90}) compared to samples from interglacial times (Fig. 3). This pattern, however, is
319 persistent only during the middle and late Pleistocene, from about 0.9 Ma until the Recent,
320 whereas there is no such clear relation in older parts of the record.

There are different possibilities to explain the observed negative correlation on glacial to interglacial time scales between the coarse dust data from Site U1467 and published dust records from the Arabian Sea. First, dust transport paths, controlled by the wind regime over the northern Indian Ocean are different during glacial times in reaction to altered northern hemisphere temperature gradients and precipitation patterns. This would potentially allow less dust to reach the Maldives. Second, the transport mechanisms responsible for the transport of coarse dust could be weaker during glacials. Beside dust entrainment, such mechanisms must ensure the continuous re-suspension of larger particles to avoid gravitational settling and to prolong transport distances. Coarse dust transport over the Arabian Sea has been shown to be linked with the strength of north-westerly Shamal winds (Sirocko and Sarnthein, 1989; Clemens, 1998; Ackerman and Cox, 1989; Nair et al., 1989; Glennie et al., 2002; Ramaswamy et al., 2017; Banerjee et al., 2019). In the Atlantic, the transport of coarse and giant African dust particles as far as the Caribbean Sea has been proposed to be linked to the occurrence of convective storm systems, which ensure deep atmospheric convection of dust particles and ensures prolonged transport (Prospero et al., 1970; Betzer et al. 1988; van der Does et al., 2018; Lindhorst et al., 2019). Similar mechanisms are imaginable for the transport of coarse dust to the Maldives, roughly 3000 km away from the potential dust sources in northeast Africa and the Arabian Peninsula. Less frequent occurrence of convective storms during glacial times, potentially as the result of lower sea-surface temperatures, would result in the observed fining of the coarse dust from Site U1467.

The negative correlation of the geochemical dust records from the Maldives (Bunzel et al., 2017; Kunkelova et al., 2018) and the coarse dust record as presented in this study is seen to result from different particle-size ranges: Element ratios were measured by XRF scanning of complete cores and as such are expected to be dominated by the mud fraction of the sediments, especially clay minerals and fine dust particles. Grain-size data of the terrigenous residue as presented in this study, by contrast, only incorporate particles in the size range 8 to 63 µm and does not take into account finer dust particles. Fine dust particles are nowadays enriched in north-easterly winter monsoonal winds (Eck et al., 2001; Chowdhury et al., 2001; Stone et al., 2007; Adhikary et al., 2007; Das et al., 2011). In addition, the West India Coastal Current (WICC), transports large water- and suspended sediment masses from the Bay of Bengal into the south-eastern Arabian Sea during the winter monsoon (Shetye, 1998; Shankar et al., 2002; Kurian and Vinayachandran, 2007; Fig. 1). Bulk terrigenous records, dominated by particles in the clay and fine silt range, are therefore prone to changes in the winter monsoon. Coarse dust particles, by contrast, are predominantly deposited during the summer

355 monsoon and periods of north-westerly Shamal winds (Clemens, 1998; Ramaswamy et al.,
356 2017; Banerjee et al., 2019). These particles are therefore expected to originate most likely
357 from dust source areas towards the west and northwest, namely northeast Africa and the
358 Arabian Peninsula.

359 To summarize, grain-size data of the terrigenous medium to coarse silt fraction (8-63 μm)
360 of Site U1467 sediments are interpreted to reflect i) the amount of transported coarse dust as
361 controlled by source area aridity and/or transport paths; and ii) the dust transport capacity as
362 controlled by the transport mechanisms, i.e. wind intensity of the Shamal wind system and/or
363 occurrence of convective storm systems. Based on the data available, a particle-size
364 dependent source is proposed for the terrigenous material deposited in the Maldives carbonate
365 drifts. Particles in the clay and fine silt range derive from rivers draining into the Bay of
366 Bengal, from where they are transported westward by the WICC during the winter monsoon.
367 By contrast, coarse dust particles likely originate from dust sources in northeast Africa and the
368 Arabian Peninsula. For these particles, a mid-tropospheric transport is proposed, initiated by
369 the north-westerly winds of the Shamal wind system which override the south-westerly winds
370 of the summer monsoon (Clemens, 1998; Ackerman and Cox, 1989; Nair et al., 1989;
371 Ramaswamy et al., 2017; Banerjee et al., 2019). As such, the grain-size data from IODP Site
372 U1467 are seen to record the variability in coarse-dust transport during the summer monsoon,
373 whereas geochemical records from the same site reflect the variability of fine particle input by
374 winter monsoonal winds and riverine input from the Bay of Bengal.

375 The proposed particle-size dependence of dust provenance has also implications for the
376 study of dust source areas based on radiogenic isotopes, like e.g. strontium and neodymium
377 isotope ratios, which are established proxies for terrigenous sediment provenance, including
378 marine sediments from the Indian Ocean (Goldstein and Jacobsen, 1987; Colin et al., 1999;
379 Jung et al., 2004; Ahmad et al., 2005; Goswami et al., 2012; Sharifi et al., 2018). Strontium
380 and neodymium isotope ratios address the provenance of bulk terrigenous material. In the fine
381 fraction the isotopic signal is due to the host minerals of Sr and Nd (zircon, monazite/allanite,
382 clay minerals, titanite and biotite), which are in the clay- to silt-sized fraction of the sediment
383 (Innocent et al., 2000; Meyer et al., 2011). Aeolian sediment provenances based on bulk-
384 terrigenous isotope ratios therefore has to be treated with caution as fine and coarse dust do
385 not necessarily originate from the same sources nor follow the same transport paths.

386

387 **5.3 Four million years of dust transport over the northern Indian Ocean**

Grain-size data from the terrigenous residue of Site U1467 sediments provide a four million year record of coarse dust transport over the northern Indian Ocean, a key area for the understanding of long-term changes in the South Asian wind systems.

The amount of coarse dust that reached the Maldives Inner Sea increased on the long-term since 4 Myr ago ($TF_{\%8-63}$; Fig. 3). The strongest increase occurred between 4.0 to 3.3 Ma. Dust transport capacity, as mirrored by the size of the largest dust particles (TF_{d90}), increased at the beginning of the record, between 4.0 to 3.3 Ma, as such paralleling the increase in the amount of coarse dust. In addition, the coarsest particles of the record, indicating highest transport intensities during the last 4 Myr, are found around 3.3 Ma.

Both, the increase in dust flux as well as of transport capacity are synchronous with the closure of the Indonesian seaway (4 to 3 Ma) and the resulting long-term cooling of ocean surface waters in the Indian Ocean (Rodgers et al., 2000; Cane and Molnar, 2001). The resulting reorganization in ocean- and atmospheric circulation is assumed to be the trigger of the late Pliocene aridification in northeast Africa and other circum-North Indian Ocean dust source areas, as well as occurred synchronous to the intensification of the South Asian Monsoon (Cane and Molnar, 2001; Zhang et al., 2009; Sun et al., 2010; Anderson et al., 2019). Both processes could have increased dust flux to the Maldives on the long-term.

From 3.3 to around 3.1 Ma grain-size data show a rapid decrease in dust flux and transport capacity. This event occurs simultaneously to the mid-Pliocene warm period; a time characterized by sea-surface temperatures 2.7 to 4 °C higher than today (mPWP; 3.3-3.0 Ma; Haywood et al., 2016). Higher sea-surface temperatures are likely to have increased precipitation in the dust source regions (Goddard and Graham, 1999; Rodgers et al., 2000), resulting in less dust export. However, the coarsening of TF_{d90} between 3.1 and 3.0 Ma and the elevated values for dust flux at the same time, indicate that dust transport over the northern Indian Ocean was not uniformly reduced during the mPWP.

Between 3.0 and 1.6 Ma, dust transport capacity is variable but decreases over the long-term. Dust flux at the same time shows no clear trend, but a temporary increase between 2.2 and 1.8 Ma. The global climate past 3.0 Ma is characterized by northern hemisphere cooling and the onset of extended glaciations (starting around 2.7 Ma, Shackleton et al., 1984; Haug et al., 1999). More locally, in the Indian Ocean dust source regions, the long-term aridification, which started around 4.0 Ma, intensified as indicated by numerous records from east Africa, where former forest and grassland areas diminished during this period (deMenocal, 1995, 2004, 2005; Cane and Molnar, 2001; Sun et al., 2010; Nie, 2017). With regard to coarse dust,

these changes in vegetation would corroborate the observed overall increase in dust flux during the last 2.4 Myr. By contrast, Arabian Sea and northern Indian Ocean wind systems, as mirrored by dust transport capacity, show no clear trend during this time. This underlines the role of source area aridity for dust flux, and as such points to a decoupling of dust flux rate from the size of transported dust particles, as described from dust records elsewhere (Clemens and Prell, 1990; Lindhorst et al., 2019).

During the last 1.6 Myr there is an increase in dust flux again, whereas transport capacity remained at a low level until the onset of the mid-Pleistocene transition (MPT; 1.25-0.75 Ma; Clark et al., 2006). During the MPT, there is no clear trend in both dust records from Site U1467. However, with the onset of the pronounced Pleistocene glacial-interglacial variability, past 0.9 Ma, the amplitude of changes in both, dust flux and dust transport capacity, increased paired with elevated dust flux rates and a coarsening of the dust grain-size spectrum. In the late Quaternary, since around 500 ka, peak dust-flux rates are higher than during any other time in the last 4 Myr.

5.4 Cyclic variability of dust transport

The visual inspection of the terrigenous grain-size data implies periodic changes of dust flux rate and dust transport capacity (Fig. 3). This is supported by wavelet spectra, which show a cyclic variability of $TF_{\%8\text{-}63}$ and TF_{d90} on orbital timescales (Fig. 4).

Higher frequency orbital-driven cycles in the precessional (23 kyr) and the obliquity (41 kyr) band are more pronounced in the variability of the particle size (TF_{d90}), than in the percentage of coarse particles ($TF_{\%8\text{-}63}$), indicating that the dust transport mechanisms (wind systems) are more prone to higher frequency orbital-driven climatic changes than the total dust flux, which is controlled by long-term changes of source-area precipitation. This interpretation stands in line with previous studies, which showed the prevalence of precessional and obliquity controlled variability in summer insolation on the strength of the South Asian Monsoon system, whereas dust flux rates are dominated by the longer periodicity of glacial-interglacial climate changes, suggesting a link to high-latitude climate variability (deMenocal, 1995; Clemens et al., 1996; Clemens, 1998; Sun et al., 2010; Bunzel et al., 2017; Nie, 2017). This, however, stands in contrast to a very recent study, which suggests that dust flux from the Sahara rather follows a precessional variability than changes on glacial-interglacial timescales (Skonieczny et al., 2019).

Low-frequency orbital-driven cyclicities in the Site U1467 dust records encompass the two eccentricity cycles with wavelengths of 100 and c. 400 kyr. The short eccentricity cycle is present in both grain-size records past 2.0 Ma, whereas it remains speculative beforehand. The influence of the short eccentricity weakens between 1.6 and 1.0 Ma (dust flux) and 1.3 and 1.0 Ma (transport capacity), respectively. The long eccentricity cycle seems to influence both, dust flux rate and transport capacity. However its influence on the dust flux rate is weak prior to 2.0 Ma, whereas it persists throughout the record if only transport capacity is considered.

6. Conclusions

Carbonate drift sediments at IODP Site U1467 from the Maldives Inner Sea provide an archive of coarse dust transport over the northern Indian Ocean during the last 4 million years. Based on grain-size data of the terrigenous residue, variability in dust flux and wind transport capacity has been reconstructed. Dust flux and wind transport capacity increased between 4.0 and 3.3 Ma, as such paralleling the closure of the Indonesian seaway and the resulting reorganization of the wind- and precipitation regime of the western Indian Ocean. In this context, the increase in grain size is interpreted to indicate an intensification of transport capacity, i.e. higher wind speeds in the north-westerly Shamal winds and/or more frequent convective storms, whereas the increase in dust flux points to more arid conditions in the dust source areas, primarily in northeast Africa and the Arabian Peninsula. Subsequently, there is variability but no clear trend in dust flux between 3.3 and 1.6 Ma, whereas transport capacity decreased during this period. Between 1.6 and the Recent, dust flux increased and shows higher variability, especially since 500 ka. Transport capacity reached a low around 1.2 Ma and increased until 500 ka. Since then, transport capacity slightly decreased.

Frequency analysis shows that coarse dust transport varies on orbital timescales, with the eccentricity control being the most prominent. Higher frequencies, as the result of changes in obliquity and precession, are more pronounced in the record of wind transport capacity than in the amount of coarse dust. This indicates that the transport of coarse dust to the Maldives as a far field site is more prone to changes in mechanisms (i.e. intensity of the Shamal winds, occurrence of convective storm systems, direction of transport) than to environmental changes in the dust source areas (precipitation rates, vegetation coverage).

Acknowledgements

The authors would like to thank the International Ocean Discovery Programm (IODP) for providing samples and data and the crew, scientific staff and shipboard science party of Joides Resolution for making Exp. 359 possible. Jutta Richarz (University of Hamburg) is thanked for chemical sample treatment and grain-size measurements, and Max Bohlen, Catalina Vulpe, and Anna-Lena Geßner for sample preparation. Liviu Giosan (Woods Hole Oceanographic Institution) is thanked for discussions on sediment provenance and radiogenic isotopes. The manuscript has been significantly improved by the detailed and thorough reviews made by two anonymous reviewers.

Data availability

Grain-size statistics for samples from Site U1467 are available from the data depository PANGAEA: doi: XXX (*will be added once available*). For grain-size parameters presented in this manuscript see supplementary material.

REFERENCES

Ackerman, S.A. and Cox, S.K., 1989. Surface weather observations of atmospheric dust over the southwest summer monsoon region. Meteorology and Atmospheric Physics, 41, 19-34.

Adhikary,B., Carmichael,G.R., Tang,Y., Leung,L.R., Qian,Y., Schauer,J.J., Stone,E.A., Ramanathan,V., Ramana,M.V., 2007. Characterization of the seasonal cycle of south Asian aerosols: A regional-scale modelling analysis. Journal of Geophysical Research, 112, D22S22.

Ahmad, S.M., Anil Babu, G., Padmakumari, V.M., Dayal, A.M., Sukhija, B.S., Nagabhushanam, P., 2005. Sr, Nd isotopic evidence of terrigenous flux variations in the Bay of Bengal: Implications of monsoons during the last ~34,000 years. Geophysical Research Letters 32, 1-4.

Anderson, C.H., Murray, R.W., Dunlea, A.G., Giosan, L., Kinsley, C.W., McGee, D., Tada, R., 2019. Aeolian delivery to Ulleung Basin, Korea (Japan Sea), during development of the

East Asian Monsoon through the last 12 Ma. Geological Magazine, doi.org/10.1017/S001675681900013X.

Aubert, O. and Droxler, A.W., 1992. General Cenozoic evolution of the Mal-dives carbonate system (equatorial Indian Ocean). Bulletin des Centres de Recherches Exploration-Production Elf-Aquitaine, 16, 113-136.

Banerjee, P., Satheesh, S.K., Moorthy, K.K., Nanjundiah, R.S., Nair, V.S., 2019. Long-range transport of mineral dust to the northeast Indian Ocean: Regional versus remote sources and the implications. Journal of Climate, 32, 1525-1549.

Betzer, P.R., Carder, K.L., Duce, R.A., Merrill, J.T., Tindale, N.W., Uematsu, M., Costello, D.K., Young, R.W., Feely, R.A., Breland, J.A., Bernstein, R.E., Greco, A.M., 1988. Long-range transport of giant mineral aerosol-particles. Nature, 336, 568-571.

Betzler, C., Hübscher, C., Lindhorst, S., Reijmer, J.J.G., Römer, M., Droxler, A.W., Fürstenau, J., and Lüdmann, T., 2009. Monsoon-induced partial carbonate platform drowning (Maldives, Indian Ocean). Geology, 37, 867-870.

Betzler, C., Fürstenau, J., Lüdmann, T., Hübscher, C., Lindhorst, S., Paul, A., Reijmer, J.J.G., and Droxler, A.W., 2013a. Sea-level and ocean-current control on carbonate-platform growth, Maldives, Indian Ocean. Basin Research, 25, 172-196.

Betzler, C., Lüdmann, T., Hübscher, C., and Fürstenau, J., 2013b. Current and sea-level signals in periplatform ooze (Neogene, Maldives, Indian Ocean). Sedimentary Geology, 290, 126-137.

Betzler, C., Eberli, G.P., Kroon, D., Wright, J.D., Swart, P.K., Nath, B.N., Alvarez-Zarikian, C.A., Alonso-Garciá, M., Bialik, O.M., Blättler, C.L., Guo, J.A., Haffen, S., Horozal, S., Inoue, M., Jovane, L., Lanci, L., Laya, J.C., Mee, A.L.H., Lüdmann, T., Nakakuni, M., Niino, K., Petruny, L.M., Pratiwi, S.D., Reijmer, J.J.G., Reolid, J., Slagle, A.L., Sloss, C.R., Su, X., Yao, Z., Young, J.R., 2016. The abrupt onset of the modern South Asian Monsoon winds. Scientific Reports 6, 1-10.

Betzler, C., Eberli, G., Alvarez Zarikian, C., Alonso-García, M., Bialik, O., Blättler, C., Guo, J., Haffen, S., Horozal, S., Inoue, M., Jovane, L., Kroon, D., Lanci, L., Laya, J., Ling Hui Mee, A., Lüdmann, T., Nakakuni, M., Nath, B., Niino, K., Petruny, L., Pratiwi, S., Reijmer, J., Reolid, J., Slagle, A., Sloss, C., Su, X., Swart, P., Wright, J., Yao, Z., Young, J., 2017. Expedition 359 summary. Proceedings of the International Ocean Discovery Program. doi: 10.14379/iodp.proc.359.101.2017.

546 Betzler, C., Eberli, G.P., Lüdmann, T., Reolid, J., Kroon, D., Reijmer, J.J.G., Swart, P.K.,
547 Wright, J., Young, J.R., Alvarez-Zarikian, C., Alonso-García, M., Bialik, O.M., Blättler, C.L.,
548 Guo, J.A., Haffen, S., Horozal, S., Inoue, M., Jovane, L., Lanci, L., Laya, J.C., Hui Mee, A.L.,
549 Nakakuni, M., Nath, B.N., Niino, K., Petruny, L.M., Pratiwi, S.D., Slagle, A.L., Sloss, C.R.,
550 Su, X., Yao, Z., 2018. Refinement of Miocene sea level and monsoon events from the
551 sedimentary archive of the Maldives (Indian Ocean). Progress in Earth and Planetary Science
552 5, 1-18.

553 Blott, S.J. and Pye, K., 2001. GRADISTAT: a grain size distribution and statistics package
554 for the analysis of unconsolidated sediments. Earth Surface Processes and Landforms, 26,
555 1237-1248.

556 Boardman, M. R., Neumann, A. C., Baker, P. A., Dulin, L. A., Kenter, R. J., Hunter, G. E.,
557 Kiefer, K. B., 1986, Banktop responses to Quaternary fluctuations in sea level recorded in
558 periplatform sediments Geology, 14, 28-31.

559 Bunzel, D., Schmiedl, G., Lindhorst, S., Mackensen, A., Reolid, J., Romahn, S., Betzler, C.,
560 2017. A multi-proxy analysis of Late Quaternary ocean and climate variability for the
561 Maldives, Inner Sea. Climate of the Past, 13, 1791-1813.

562 Cane, M.A. and Molnar, P., 2001. Closing of the Indonesian seaway as a precursor to east
563 African aridification around 3-4 million years ago. Nature, 411, 157-162.

564 Chowdhury, Z., Hughes, L.S., Salmon, L.G., 2001. Atmospheric particle size and
565 composition measurements to support light extinction calculations over the Indian Ocean.
566 Journal of Geophysical Research, 106, D22, 28597-28605.

567 Clark, P.U., Archer, D., Pollard, D., Blum, J.D., Rial, J.A., Brovkin, V., Mix, A.C., Pisias,
568 N.G., Roy, M., 2006. The middle Pleistocene transition: characteristics, mechanisms, and
569 implications for long-term changes in atmospheric pCO2. Quaternary Science Reviews, 25,
570 3150-3184.

571 Clemens, S.C. and Prell, W.L., 1990. Late Pleistocene variability of Arabian Sea summer
572 monsoon winds and continental aridity: eolian records from the lithogenic component of
573 deep-sea sediments. Paleoceanography, 5, 109-145.

574 Clemens, S., Prell, W., Murray, D., Shimmield, G., Weedon, G., 1991. Forcing mechanisms
575 of the Indian Ocean monsoon. Nature, 353, 720-725.

576 Clemens, S.C.,Murray, D.W., Prell, W.L., 1996. Nonstationary Phase of the Plio-Pleistocene
577 Asian Monsoon. Science, 274, 943-948.

578 Clemens, S.C., 1998. Dust response to seasonal atmospheric forcing: Proxy evaluation and
579 calibration. Paleoceanography, 13, 471-490.

580 Colin, C., Turpin, L., Bertaux, J., Desprairies, A., Kissel, C., 1999. Erosional history of the
581 Himalayan and Burman ranges during the last two glacial-interglacial cycles. Earth and
582 Planetary Science Letters 171, 647-660.

583 Das, R., Granat, L., Leck, C., Praveen, P.S., 2011. Chemical composition of rainwater at
584 Maldives Climate Observatory at Hanimaadhoo (MCOH). Atmospheric Chemistry and
585 Physics, 11, 3743-3755.

586 deMenocal, P., 2005. Plio-Pleistocene African climate. Science, 270, 53-59.

587 deMenocal, P., 2004. African climate change and faunal evolution during the Pliocene-
588 Pleistocene. Earth and Planetary Science Letters, 220, 3-24.

589 van der Does, M., Knippertz, P., Zschenderlein, P., Giles Harrison, R., Stuut, J.-B., 2018. The
590 myterious long-range transport of giant mineral dust particles. Science Advances, 4,
591 eaau2768.

592 Droxler, A.W., Haddad, G.A., Mucciarone, D.A., and Cullen, J.L., 1990. Pliocene-Pleistocene
593 aragonite cyclic variations in Holes 714A and 716B (The Maldives) compared with Hole
594 633A (The Bahamas): records of climate-induced $CaCO_3$ preservation at intermediate water
595 depths. In: Duncan, R.A., Backman, J., Peterson, L.C., et al. (Eds), Proceedings of the Ocean
596 Drilling Program, Scientific Results, 115, 539-577.

597 Eck, T.F., Holben, B.N., Dubovik, O., Smirnov, A., Slutsker, I., Lobert, J.M., Ramanathan,
598 V., 2001. Column-integrated aerosol optical properties over the Maldives during the northeast
599 monsoon for 1998-2000. Journal of Geophysical Research, 106, 28555-28566.

600 Folk, R.L. and Ward, W.C., 1957. Brazos River bar; a study in the significance of grain size
601 parameters. Journal of Sedimentary Research, 27, 3-26.

602 Glaser, K. S., and Droxler, A. W., 1993, Controls and development of Late Quartenary
603 periplatform carbonate stratigraphy in Walton Basin (Northeastern Nicaragua Rise,
604 Carribbean Sea). Paleoceanography, 8, 243-274.

605 Glennie, K.W., Singhvi, A.K., Lancaster, N., Teller, J.T., 2002. Quaternary climatic changes
606 over Southern Arabia and the Thar Desert, India. In: Clift, P.D., Kroon, D., Gaedicke, C.,
607 Craig, J. (Eds), The Tectonic and Climatic Evolution of the Arabian Sea Region. Geological
608 Society, London, Special Publications, 195, 301-316.

609 Goddard, L. and Graham, N.E., 1999. Importance of the Indian Ocean for simulating rainfall
610 anomalies over eastern and southern Africa. Journal of Geophysical Research, 104, 19099-
611 19116.

612 Goswami, V., Singh, S.K., Bhushan, R., Rai, V.K., 2012. Temporal variations in $^{87}Sr/^{86}Sr$ and
613 □Nd in sediments of the southeastern Arabian Sea: Impact of monsoon and surface water
614 circulation. Geochemistry, Geophysics, Geosystems, 13, Q01001.

615 Gupta, A.K., Anderson, D.M., Overpeck, J.T., 2003. Abrupt changes in the Asian southwest
616 monsoon during the Holocene and their links to the North Atlantic Ocean. Nature 421, 354-
617 357.

618 Gupta, A.K., Yuvaraja, A., Prakasam, M., Clemens, S.C., Velu, A., 2015. Evolution of the
619 South Asian monsoon wind system since the late Middle Miocene. Palaeogeography,
620 Palaeoclimatology, Palaeoecology 438, 160-167.

621 Hammer, Ø., Harper, D.A.T., Ryan, P.D., 2001. PAST: paleontological statistics software
622 package for education and data analysis. Palaeontologia Electronica, 4, 9 pp.

623 Haug, G.H., Sigman, D.M., Tiedemann, R., Pedersen, T.F., Sarnthein, M., 1999. Onset of
624 permanent stratification in the subarctic Pacific Ocean. Nature, 401, 779-782.

625 Haywood, A.M., Dowsett, H.J., Dolan, A.M., 2016. Integrating geological archives and
626 climate models for the mid-Pliocene warm period. Nature Communication, 7, 10646.

627 Huybers, P. and Eisenman, I., 2006. Integrated summer insolation calculations. IGBP
628 PAGES/World Data Center for Paleoclimatology Data Contribution Series # 2006-079.
629 NOAA/NCDC Paleoclimatology Program, Boulder CO, USA.

630 Innocent, C., Fagel, N., Hillaire-Marcel, C., 2000. Sm-Nd isotope systematics in deep-sea
631 sediments: clay-size versus coarser fractions. Marine Geology 168, 79-87.

632 Jung, S.J.A., Davies, G.R., Ganssen, G.M., Kroon, D., 2004. Stepwise Holocene aridification
633 in NE Africa deduced from dust-borne radiogenic isotope records. Earth and Planetary
634 Science Letters, 221, 27-37.

635 Kessarkar, P.M., Rao, V.P., Ahmad, S.M., Babu, G.A., 2003. Clay minerals and Sr-Nd
636 isotopes of the sediments along the western margin of India and their implication for sediment
637 provenance. Marine Geology 202, 55-69.

638 Kolla, V., Kostecki, J., Robinson, F., Biscaye, P., Ray, P., 1981. Distribution and origins of
639 clay minerals and quartz in surface sediments of the Arabian Sea. Journal of Sedimentary
640 Research, 51, 563-569.

641 Kroon, D., Steens, T., Troelstra, S.R., 1991. Onset of monsoonal related upwelling in the
642 western Arabian Sea as revealed by planktonic foraminifers. In: Prell, W.L., Niitsuma, N., et
643 al., (Eds), Proceedings of the Ocean Drilling Program, Scientific Results, 117, 257-263.

644 Kunkelova, T.; Jung, S., de Leau, E., Odling, N., Thomas, A., Betzler, C., Eberli, G., Alvarez-
645 Zarikian, C., Alonso-García, M., Bialik, O., Blättler, C., Guo, J., Haffen, S., Horozal, S., Ling
646 Hui Mee, A.; Inoue, M., Jovane, L., Lanci, L., Laya, J., Lüdmann, T., Nath, N., Nakakuni, M.,
647 Niino, K., Petruny, L., Pratiwi, S., Rijmer, J., Reolid, J., Slagle, A., Sloss, C., Su, X., Swart,
648 P., Wright, J., Yao, Z., Young, J., Lindhorst, S., Hayman-Stainbank, S., Rüggeberg, A.,
649 Spezzaferri, S., Carrasqueira, I., Yu, S., Kroon, D., 2018. A two million year record of low
650 latitude aridity linked to continental weathering from the Maldives. Progress in Earth and
651 Planetary Science, 5, 86.

652 Kurian, J. and Vinayachandran, P.N., 2007. Mechanisms of formation of the Arabian Sea
653 mini warm pool in a high-resolution Ocean General Circulation Model. Journal of
654 Geophysical Research, 112: C05009.

655 Lanci, L., Zanella, E., Jovane, L., Alonso-García, M., Alvarez-Zarikian, C.A., Betzler, C.,
656 Bialik, O.M., Blättler, C.L., Eberli, G.P., Guo, J.A., Haffen, S., Horozal, S., Inoue, M., Kroon,
657 D., Laya, J.C., Ling Hui Mee, A., Lüdmann, T., Nakakuni, M., Bejugam, N.N., Niino, K.,
658 Petruny, L.M., Pratiwi, S.D., Reijmer, J.J.G., Reolid, J., Slagle, A.L., Sloss, C.R., Su, X.,
659 Swart, P.K., Wright, J.D., Yao, Z., Young, J.R., submitted. Magnetic properties of Early
660 Pliocene sediments from IODP Site 2U1467 (Maldives platform) reveal changes in the
661 monsoon system. Palaeogeography, Palaeoclimatology, Palaeoecology.

662 Laskar, J., P. Robutel, F. Joutel, M. Gastineau, A.C.M. Correia, B. Levrard, 2004. A long-
663 term numerical solution for the insolation quantities of the Earth. Astronomy and
664 Astrophysics 428, 261-285.

665 Léon, J.-F. and Legrand, M., 2003. Mineral dust sources in the surrounding of the north
666 Indian Ocean. Geophysical Research Letters, 30, 1309.

667 Lisiecki, L. E. and Raymo, M.E., 2005, A Pliocene-Pleistocene stack of 57 globally
668 distributed benthic d18O records, Paleoceanography, 20, PA1003.

669 Lindhorst, S., Betzler, C., Wunsch, M., Lüdmann, T., Kuhn, G., 2019. Carbonate drifts as
670 marine archives of aeolian dust (Santaren Channel, Bahamas). Sedimentology, doi:
671 10.1111/sed.12576

672 Lüdmann, T., Kalvelage, C., Betzler, C., Fürstenau, J., Hübscher, C., 2013. The Maldives, a
673 giant isolated carbonate platform dominated by bottom currents. Marine and Petroleum
674 Geology, 43, 326-340.

675 McCave, I.N., Manighetti, B. and Robinson, S.G. 1995. Sortable silt and fine sediment
676 size/composition slicing: parameters for palaeocurrent speed and palaeoceanography.
677 Paleoceanography, 10, 593-610.

678 Meyer, I., Davies, G.R., Stuut, J.B.W., 2011. Grain size control on Sr-Nd isotope provenance
679 studies and impact on paleoclimate reconstructions: An example from deep-sea sediments
680 offshore NW Africa. Geochemistry, Geophysics, Geosystems, 12, 1-14.

681 Middleton, N.J., 1986a. A geography of dust storms in south-west Asia. Journal of
682 Climatology, 6, 183-196.

683 Middleton, N.J., 1986b. Dust storms in the Middle East. Journal of Arid Environments, 10,
684 83-96.

685 Miller, K.G., Kominz, M.A., Browning, J.V., Wright, J.D., Mountain, G.S., Katz, M.E.,
686 Sugarman, P.J., Cramer, B.S., Christie-Blick, N., Pekar, S.F., 2005. The Phanerozoic record
687 of global sea-Level change. Science, 310, 1293-1298.

688 Nair, R.R., Ittekkot, V., Manganini, S.J., Ramaswamy, V., Haake, B., Degens, E.T., Desai,
689 B.N., Honjo, S., 1989. Increased particle flux to the deep ocean related to monsoons. Nature,
690 338, 749-751.

691 Nie, J., 2017. The Plio-Pleistocene 405-kyr climate cycles. Palaeogeography,
692 Palaeoclimatology, Palaeoecology, 510, 26-30.

693 Paillard, D., Labeyrie, L., Yiou, P., 1996. Macintosh Program performs time-series analysis.
694 Eos, 77, 379.

695 Paul, A., Reijmer, J. J. G., Fürstenau, J., Kinkel, H., and Betzler, C., 2012, Relationship
696 between Late Pleistocene sea-level variations, carbonate platform morphology and aragonite
697 production (Maldives, Indian Ocean). Sedimentology, 59, 1540-1658.

698 Prell, W.L. and van Campo, E., 1986. Coherent response of Arabian Sea upwelling and pollen
699 transport to Late Quaternary monsoonal winds. Nature, 323, 526-528.

Prospero, J.M., Bonatti, E., Schubert, C., Carlson, T.N., 1970. Dust in the Caribbean atmosphere traced to an African dust storm. Earth and Planetary Science Letters, 9, 287-293.

Prospero, J.M., Ginoux, P., Torres, O., Nicholson, S.E., Gill, T.E., 2002. Environmental characterization of global sources of atmospheric soil dust identified with the Nimbus 7 Total Ozone Mapping Spectrometer (TOMS) Absorbing Aerosol product. Reviews of Geophysics, 40, 1002.

Purdy, E.G. and Bertram, G.T., 1993. Carbonate Concepts from the Maldives, Indian Ocean. AAPG Studies in Geology, 34.

Ramaswamy, V., 2014. Influence of tropical storms in the northern Indian Ocean on dust entrainment and long-range transport. In: Tang and Sui (Eds), Typhoon impact and crisis management. Advances in Natural and Technological Hazard Research, 40, 149-174.

Ramaswamy, V., Muraleedharan, P.M., Babu, P., 2017. Mid-troposphere transport of Middle-East dust over the Arabian Sea and its effect on rainwater composition and sensitive ecosystems over India. Scientific Reports, 7, 13676.

Rodgers, K.B., Latif, M., Legutke, S., 2000. Sensitivity of equatorial Pacific and Indian Ocean watermasses to the position of the Indonesian throughflow. Geophysical Research Letters, 27, 2941-2945.

Shackleton, N.J., Backman, J., Zimmerman, H., Kent, D.V., Hall, M.A., Roberts, D.G., Schnitker, D., Baldauf, J.G., Desprairies, A., Homrighausen, R., Huddlestun, P., Keene, J.B., Kaltenback, A.J., Krumsiek, K.A.O., Morton, A.C., Murray, J.W., Westberg-Smith, J., 1984. Oxygen isotope calibration of the onset of ice-rafting and history of glaciation in the North Atlantic region. Nature, 307, 620-623.

Shankar, D., Vinayachandran, P.N., Unnikrishnan, A.S., 2002. The monsoon currents in the north Indian Ocean. Progress in Oceanography 52, 63-120.

Sharifi, A., Murphy, L.N., Pourmand, A., Clement, A.C., Canuel, E.A., Beni, A.N., Lahijani, H.A., Delanghe, D., Ahmady-Birgani, H., 2018. Early-Holocene greening of the Afro-Asian dust belt changed sources of mineral dust in West Asia. Earth and Planetary Science Letters, 481, 30-40.

Shetye, S.R., 1998. West India Coastal Current and Lakshadweep High/Low. Sadhana, 23, 637-651.

730 Sirocko, F. and Sarnthein, M., 1989. Wind-borne deposits in the northwestern Indian Ocean:
731 record of Holocene sediments versus modern satellite data. In: Leinen, M. and Sarnthein, M.
732 (Eds), Paleoclimatology and Paleometeorology: Modern and Paste Pattern of Global
733 Atmospheric Transport. Kluwer Academic, Dordrecht, The Netherlands, 401-433.

734 Skonieczny, C., McGee, D., Winckler, G., Bory, A., Bradtmiller, L.I., Kinsley, C.W.,
735 Polissar, P.J., De Pol-Holz, R., Rossignol, L., Malaizé, B., 2019. Monsoon-driven Saharan
736 dust variability over the past 240,000 years. Science Advances, 5, eaav1887.

737 Stone, E.A., Lough, G.C., Schauer, J.J., Praveen, P.S., Corrigan, C.E., Ramanathan, V., 2007.
738 Understanding the origin of black carbon in the atmospheric brown cloud over the Indian
739 Ocean. Journal of Geophysical Research, 112, D22S23.

740 Sun, Y.B., An, Z.S., Clemens, S.C., Bloemendal, J., Vandenberghe, J., 2010. Seven million
741 years of wind and precipitation variability on the Chinese Loess Plateau. Earth and Planetary
742 Science Letters, 297, 525-535.

743 Tanaka TY and Chiba M, 2006. A numerical study of the contributions of dust source regions
744 to the global dust budget. Global and Planetary Change, 52, 88-104.

745 Tomczak, M. and Godfrey, J.S., 2003. Regional Oceanography: An Introduction. Daya
746 Publishing House, Delhi.

747 Tsoar, H. and Pye, K., 1987. Dust transport and the question of desert loess formation.
748 Sedimentology, 34, 139-153.

749 Wyrtki, K. (1973). Physical oceanography of the Indian Ocean. In: Zeitschel (Ed), The
750 biology of the Indian Ocean. Springer-Verlag, New York.

751 Yu, Y., Notaro, M., Kalashnikova, O.V., Garay, M.J., 2015. Climatology of summer Shamal
752 wind in the Middle East. Journal of Geophysical Research: Atmosphere, 121, 289-305.

753 Zhang, Y.G., Ji, J., Balsam, W., Liu, L., Chen, J., 2009. Mid-Pliocene Asian monsoon
754 intensification and the onset of Northern Hemisphere glaciation. Geology, 37, 599-602.

755

756 Figure Captions

757

758 **Fig. 1: A, B)** Location of the study site in the Indian Ocean; WICC: West India Coastal
759 Current during northern hemisphere winter months (after Shetye, 1998); **C)** Multibeam

760 bathymetry of the Maldives' Inner Sea surrounding the IODP expedition 359 drilling site
761 U1467. Red dot marks position of IODP site U1467.

762

763 **Fig. 2: A)** Age-depth plot for site U1467 splice section. Depths are given in metres of core
764 depth (mcd) with reference to the CCSF-359-U1467-ABCD-20160114 depth scale. Green
765 dots and named biostratigraphic events refer to the biostratigraphy as reported by Betzler et al.
766 (2017). Please note that depths of biostratigraphic tie points are midpoints depths, recalculated
767 to mcd. Grey dots are age tie points derived from correlating bulk grain-size data of U1467
768 (this work) against long-term sea-level data (Miller et al., 2005). See methods section for
769 details.

770

771 **Fig. 3: A)** Summer insolation for 65°N and sea-level data of Miller et al. (2005); **B)** Results
772 of grain-size analyses of the bulk and the terrigenous sediment fraction of site U1467
773 sediments: Percentage of bulk mud ($Bulk_{\%mud}$); percentage of terrigenous particles in the size
774 range 8-63 µm ($TF_{\%8-63}$); size of largest terrigenous particles (TF_{d90}); mean grain size of the
775 terrigenous fraction <63 µm ($TF_{Mean\ <63}$). Main global climate events are indicated for
776 orientation: Middle Pleistocene Transition (MPT; 1.25-0.75 Ma; Clark et al., 2006); mid
777 Pliocene warm period (mPWP; 3.3-3.0 Ma; Haywood et al., 2016); onset of extensive
778 northern Hemisphere glaciation (since 2.7 Ma; Shackleton et al., 1984; Haug et al., 1999);
779 closure of Indonesian seaway (4.0-3.0 Ma; Cane and Molnar, 2001).

780

781 **Fig. 4:** Wavelet spectra for the terrigenous fraction of site U1476 samples for **A)** percentage
782 of terrigenous particles falling into the 8-63 µm size range ($TF_{\%8-63}$); and **B)** size of the
783 coarsest particles (TF_{d90}).

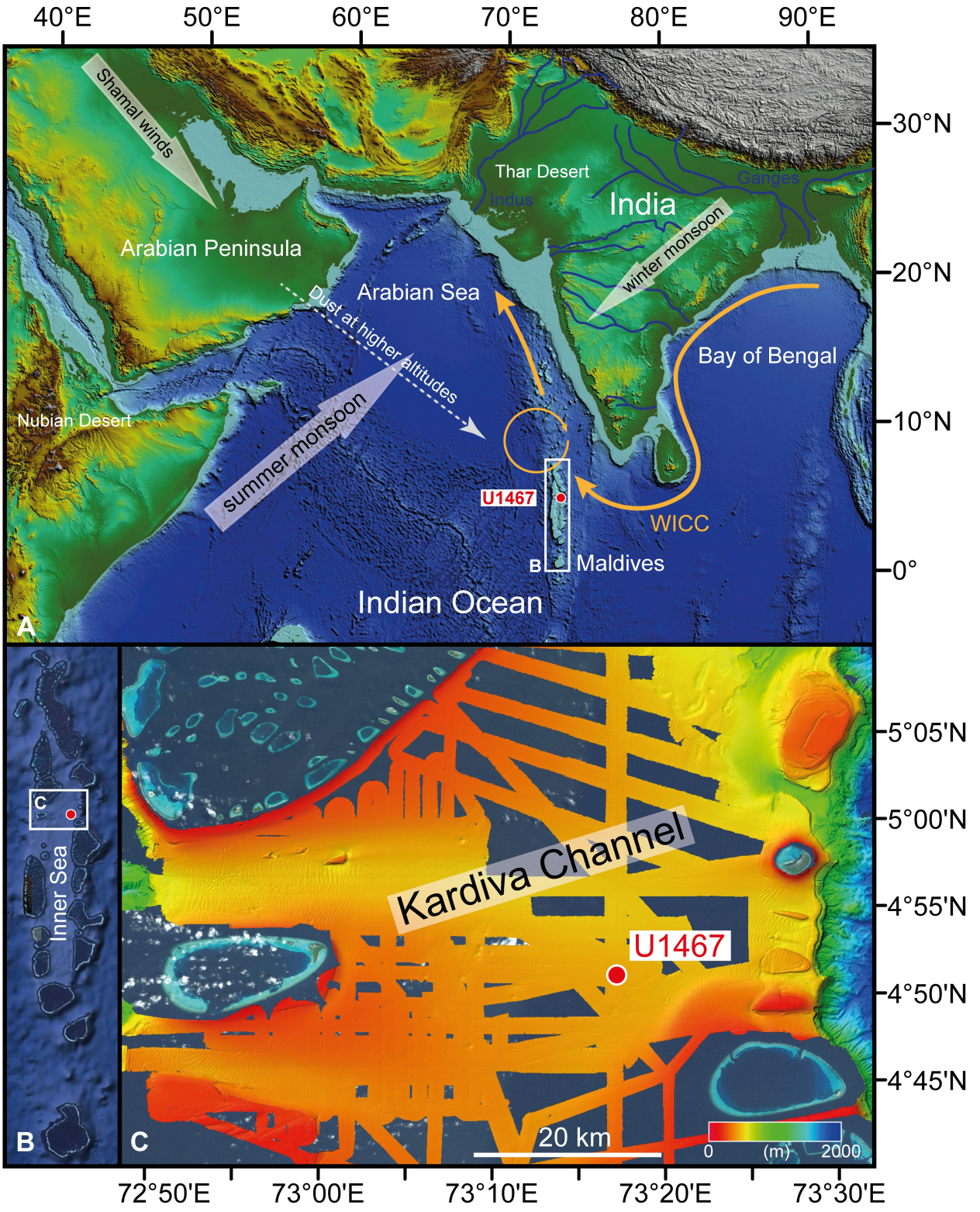

Lindhorst et al., Fig. 1

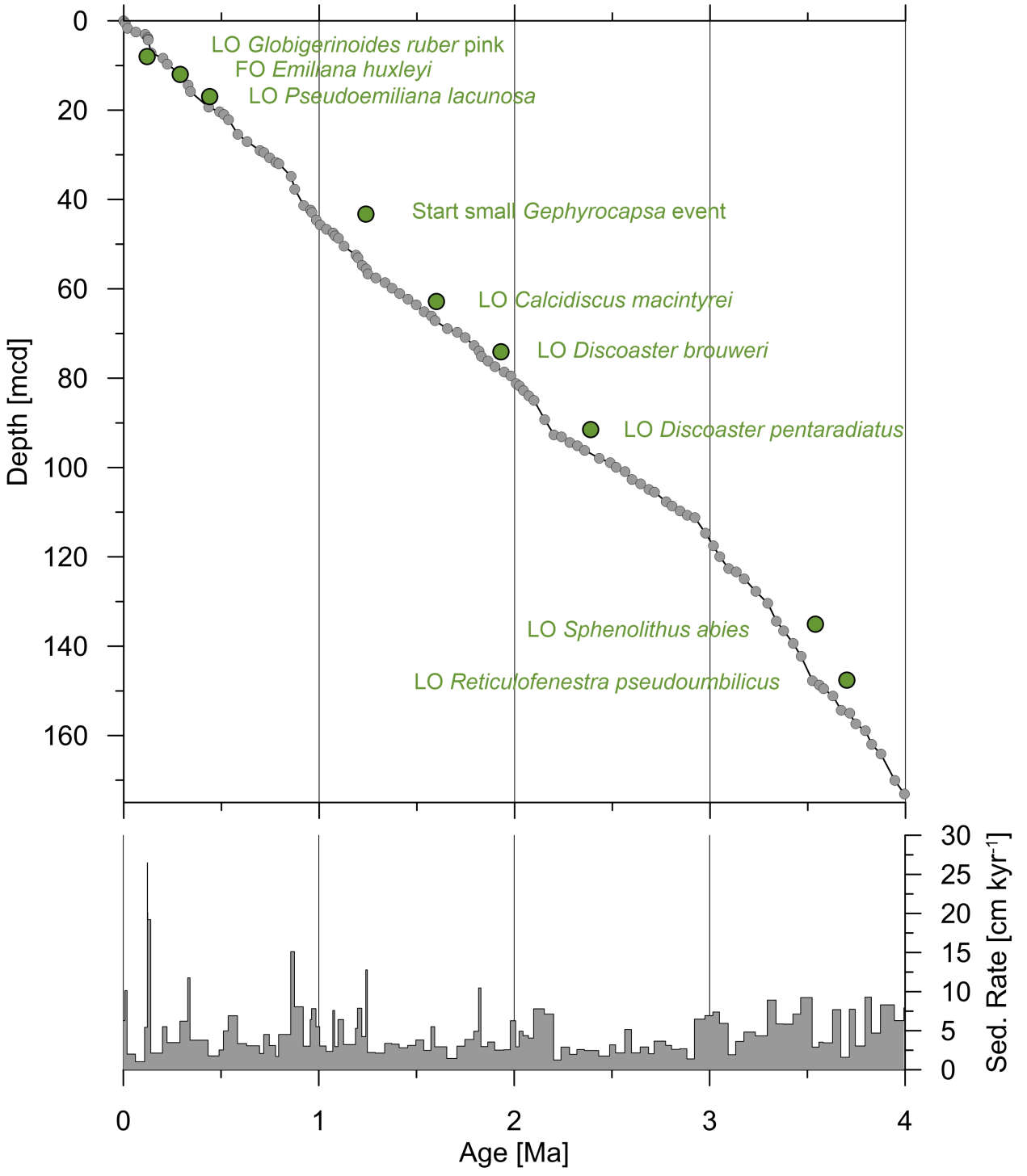

Lindhorst et al., Fig. 2

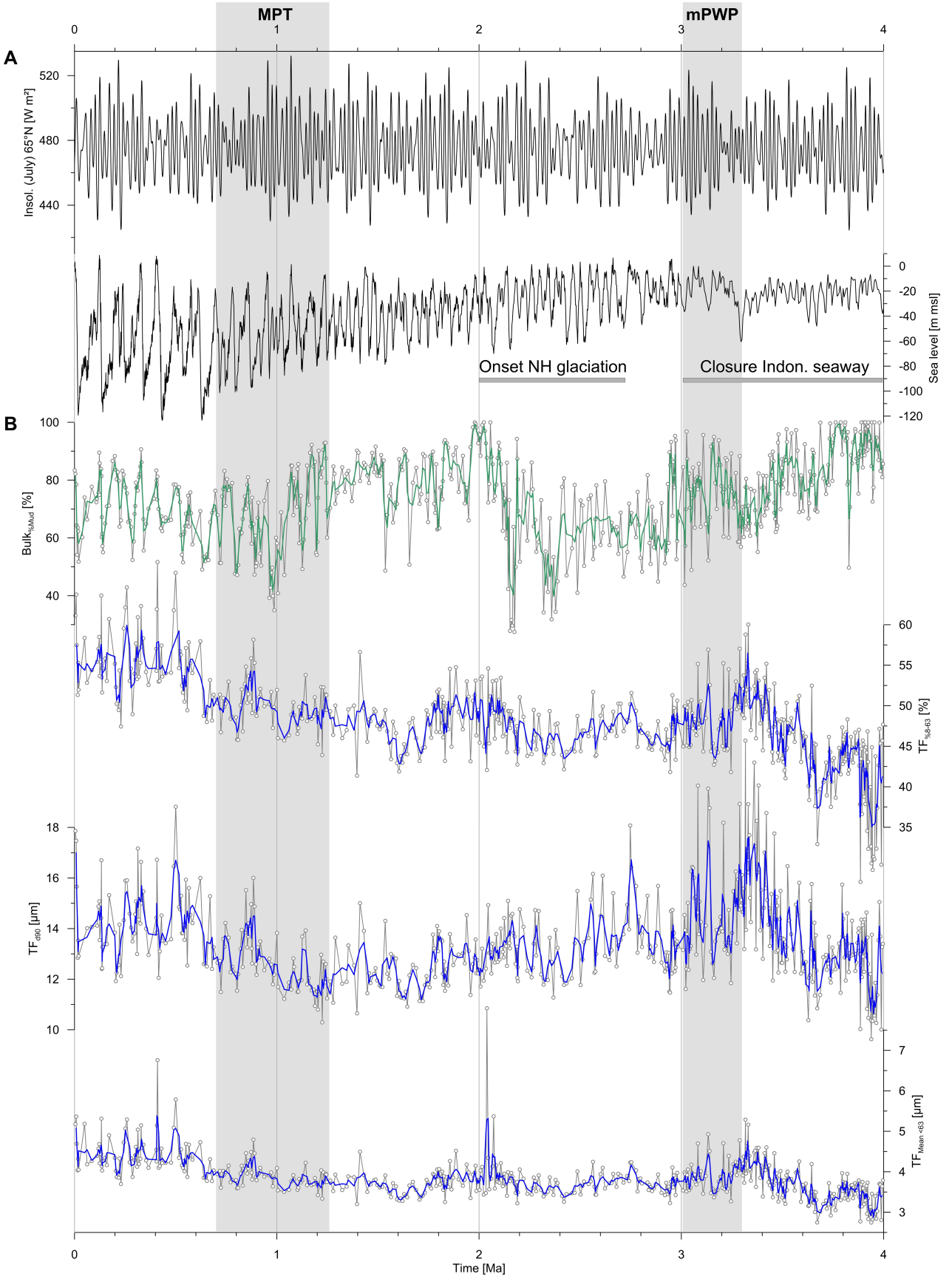

Lindhorst et al., Fig. 3

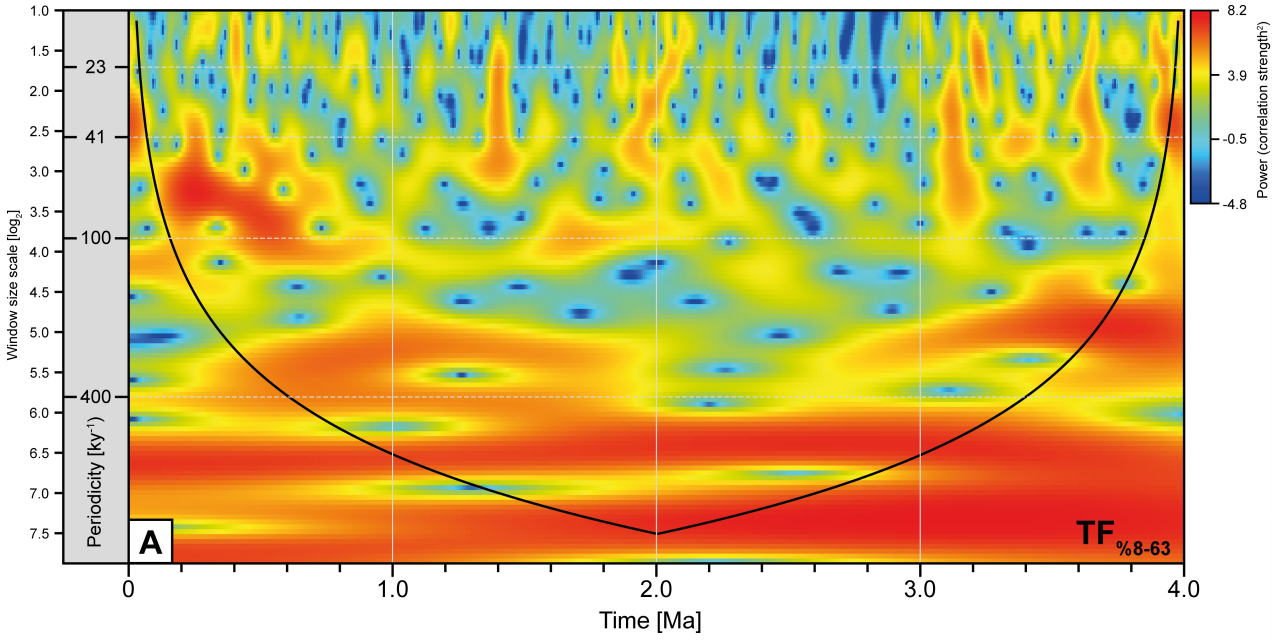

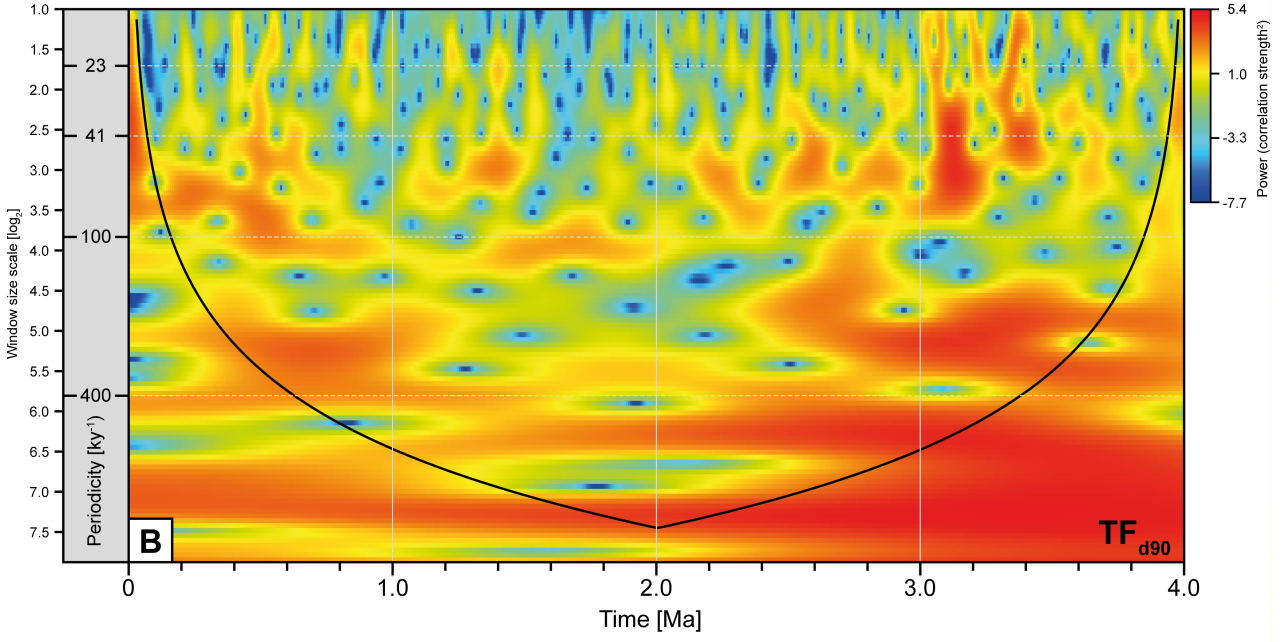

Lindhorst et al., Fig. 4